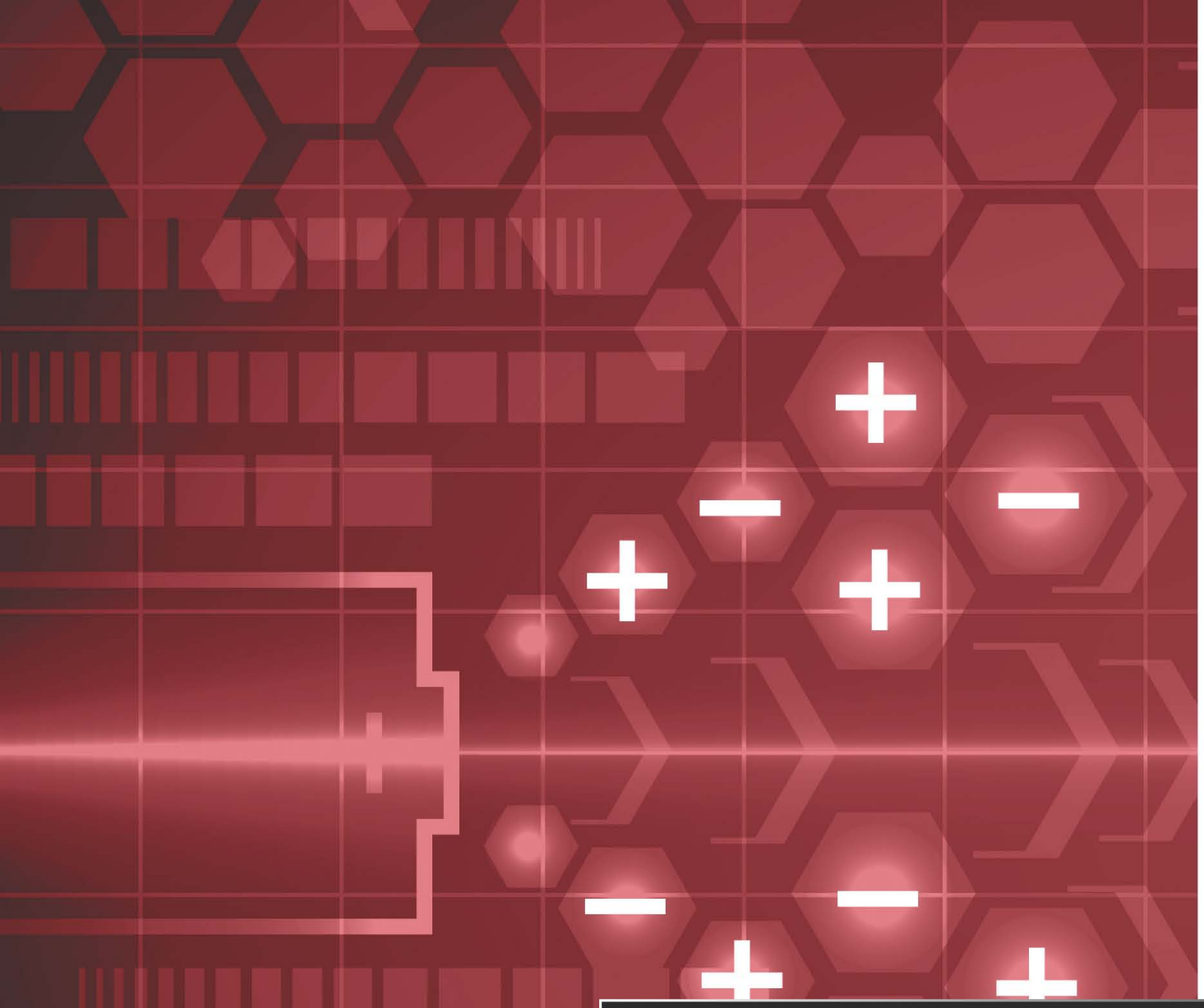

Physics-Based Methods

Gregory L. Plett
M. Scott Trimboli

ARTECH BOOKS

BATTERY MANAGEMENT SYSTEMS

VOLUME III

Battery Management Systems

Volume III

Physics-Based Methods

For a listing of recent titles in the
Artech House Power Engineering and Power Electronics,
turn to the back of this book.

Battery Management Systems

Volume III

Physics-Based Methods

Gregory L. Plett
M. Scott Trimboli

ARTECH
HOUSE
BOSTON | LONDON
artechhouse.com

Library of Congress Cataloging-in-Publication Data
A catalog record for this book is available from the U.S. Library of Congress.

British Library Cataloguing in Publication Data
A catalog record for this book is available from the British Library.

ISBN-13: 978-1-63081-904-0

Cover design by Joi Garron

685 Canton Street
Norwood, MA 02062

10 9 8 7 6 5 4 3 2 1

Contents

Preface

This book comprises the third and final volume in a series presenting battery-management systems with a particular emphasis on how to meet their algorithmic requirements. The first volume derived sets of mathematical equations (models) that describe how lithium-ion battery cells work, both internally (physics-based models) and as observed externally (empirical equivalent-circuit models). The second volume discussed state-of-the-art applications of equivalent-circuit models to solving problems in battery management and control. This third volume discusses how to use physics-based models of battery cells in a computationally efficient framework to optimize battery-pack management and control to maximize a battery pack's performance and extend its life.

The intention of the series is not to be encyclopedic; rather, it is to put forward only the current best practices with sufficient fundamental background to understand them thoroughly. This volume builds on the content in Vols. I and II. For the deepest understanding, the reader should have already studied these earlier volumes; however, we provide review material such that this third volume is generally self-contained.

Certainly, what is meant by "best practices" is at least somewhat subjective, and we may well have overlooked approaches and methodologies that are better in some applications than those described herein. Perhaps we should say, "best" from our own point of view, given what we happen to have tried, in application domains and problems we have attempted to address.

The majority of present battery-management systems still use equivalent-circuit models to aid with the computation of estimates of battery state of charge, state of health, available power, and available energy. While these methods can provide useful results, they are not able to predict the impact of battery usage on overall battery service life. Physics-based models and physics-based methods are needed to optimize the tradeoff between performance and life directly. This volume introduces and teaches the state of the art in physics-based

methods for battery management. Since this field is still very young, it additionally points out where improvements beyond the present state-of-art can still be made.

This particular volume is organized in the following way:

- Chapter 1 introduces the need for physics-based battery management and reviews the equations comprising a baseline physics-based model of lithium-ion cells. It further shows how the parameter set of the model can be reduced to enable estimating the parameter values of the model to fit a particular physical cell.
- Chapter 2 augments the baseline model with additional terms to describe the electrical double layer and constant-phase-element behaviors observed in real cells. It then develops a frequency-domain impedance model of the cell, which is useful on its own but is further needed when estimating model parameter values.
- Chapter 3 describes how to estimate the parameter values of a physics-based model using carefully designed laboratory tests. In particular, it introduces the OCP, OCV, pulse-resistance, discharge, and EIS tests, each of which is useful for producing data that can be used to estimate a subset of model parameter values. The chapter teaches lab-test procedures, data-processing procedures, and parameter-optimization methods.
- Chapter 4 shows how to convert the physics-based models discussed so far—which comprise complicated coupled partial-differential equations—into computationally simple reduced-order physics-based models. Some aspects are similar to Chap. 6 in Vol. I, but this volume introduces new, better methods and results. It further describes how to simulate constant-voltage and constant-current events with these physics-based models and how to simulate battery packs comprising multiple cells.
- Chapter 5 develops state estimators for battery-management systems using physics-based reduced-order models. These methods can produce estimates of state of charge, but more importantly can also estimate cell internal electrochemical variables as well as corresponding confidence intervals on the estimates. These estimates are necessary to be able to optimize life and performance jointly.
- Chapter 6 introduces the ideas of diagnosis and prognosis as applied to aging battery packs. A concise survey of the field is presented and several different methods are described in more detail.
- Chapter 7 employs the reduced-order models developed in Chap. 4 within the framework of model-predictive control (MPC) in order to optimize battery fast charge. In particular, it demonstrates how to charge a cell as quickly as possible without violating electro-

chemical limits that would contribute to performance degradation (e.g., lithium plating).
- Chapter 8 explains the main ideas behind battery power utilization and shows how to use MPC to compute a dynamic state of power measure, and then concludes this volume.

The intended audience for this material is someone with an undergraduate degree in engineering—principally electrical or mechanical. Readers with different backgrounds may find some of the material too basic (because they have studied it before, whereas an engineering student would not), or not descriptive enough (because they are missing some background that would typically be encountered in an engineering degree program). Both problems have a remedy, although the solution to the second involves background research to become proficient in an unfamiliar discipline—not an easy undertaking. The book also assumes that Vols. I and II are at hand, to confer for some of the background review materials.

The content of this book has been taught to students of diverse backgrounds in *ECE5730: Physics-Based Battery Management* at the University of Colorado Colorado Springs. The feedback that we received from these students has been invaluable in helping us to refine our approach to presenting these topics.

We are also greatly indebted to our colleagues and both past and present students who have assisted us over the years to understand and develop the materials presented in this work. Dr. Shriram Santhanagopalan taught us the parameter-lumping method presented in Chap. 1. Drs. Albert Rodríguez, Zhengyu Chu, and Xiangdong Kong contributed to deriving and validating the new transfer functions of Chap. 2 and rewriting them in terms of lumped parameters. Dr. Ryan Jobman, Dr. Dongliang Lu, Mr. Brandon Guest, and Mr. Wesley Hileman pioneered the parameter-estimation methods presented in Chap. 3. Dr. Albert Rodríguez was the first to implement several new realization algorithms, including the HRA presented in Chap. 4; he also pioneered output blending versus the earlier model-blending methods. Mr. Kirk Stetzel implemented earlier versions of physics-based state-estimation methods; we followed his work when developing Chap. 5. Dr. Adam Smiley was the first to apply the interacting multiple model Kalman filter to the problem of model selection, presented in Chap. 6. Mr. Aloisio Kawakita de Souza was the first to implement the physics-based thermal model also presented in Chap. 6 and engineered the implementation of combined MPC-xKF using output blending, which forms a significant contribution to Chaps. 7 and 8. Drs. Marcelo Xavier, Kiana Karami, and Gustavo Florentino also contributed foundational material to the development of MPC

methods for lithium-ion battery management presented in these two chapters.

Despite our best intentions, there are certain to be errors and confusing statements in this book. Please feel free to send us corrections and suggestions for improvements.

1
Redundant Parameter Elimination

At the time of writing, high-capacity battery systems appear to be at the threshold of a rapid acceleration in commercial adoption. Electric-vehicle market share in the United States remains low, around 2 %, but year-over-year growth is around 40 % globally at this point. Market share of plug-in vehicles in Norway is presently over 80 %, indicating that consumer acceptance of this technology can be very high. Many of the largest automakers have vowed to eliminate combustion vehicles from their product lineup this decade and many countries and regions have banned sales of new combustion vehicles by 2035 or earlier. The market for electric-drivetrain vehicles is about to be transformed.

Similarly, large-scale grid services are expanding. Utility-scale battery systems like the 150 MWh Hornsdale Power Reserve in South Australia provide grid stability and system security. Many big-box retail stores are investing in battery systems to implement peak shaving—storing electric energy during periods of the day when utility rates are low and then using the stored energy from the batteries during periods when the utility rates are high. This trend is likely to grow as the cost of batteries continue to drop and as more renewables—which have unpredictable generation capabilities—are added to the mix of power-generation means.

It is becoming increasingly more important to manage battery systems well, which is the focus of this series of volumes on battery-management systems (BMSs). The first volume[1] focused on developing models (i.e., sets of equations) that describe the dynamic behaviors of lithium-ion battery cells. These models divide into two main categories: empirical equivalent-circuit models (ECMs) and physics-based models (PBMs) developed from electrochemical and physical first principles. The second volume[2] showed how to use ECMs within battery-management algorithms to estimate cell state of charge (SOC), state of health (SOH), state of power (SOP, sometimes called state of function or SOF), and state of energy (SOE).[3] This vol-

[1] Gregory L. Plett, *Battery Management Systems, Volume 1: Battery Modeling*. Artech House, 2015.

[2] Gregory L. Plett, *Battery Management Systems, Volume 2: Equivalent-Circuit Methods*. Artech House, 2015.

[3] Collectively, these estimates are often termed "SOx."

ume shows how to use PBMs to achieve similar goals and also to enable fast charge.

Replacing ECMs with PBMs in BMS algorithms is vitally important to optimizing next-generation BMS. Why? Many battery systems that use ECM-based BMS operate very well already. Vol. II showed that BMS algorithms based on ECMs can give very good estimates of SOC, SOH, and SOE. However, ECMs predict only externally measurable cell quantities such as the terminal-voltage and surface-temperature response of a cell to an input-current stimulus. PBMs also predict these quantities but can additionally predict internal electrochemical variables such as electrical potentials, lithium concentrations, lithium fluxes, and temperatures at different spatial locations interior to a cell. This is important since the rate of cell aging depends directly on these internal variables and not on externally measurable quantities. We cannot predict the incremental degradation caused to a cell by a proposed load profile without knowing the cell's internal variables and therefore it is fundamentally impossible to optimize a tradeoff between cell performance and rate of aging directly and robustly using an ECM. If we wish to utilize a battery up to its physical limits of performance—but not beyond—then we must have good estimates of these internal variables. We must use PBM-based BMS.

This is why we believe that some form of PBM will form the basis for future BMS. As the market moves toward requirements for stricter guarantees of safety and service life and a demand for higher levels of performance, battery applications will require that the BMS compute battery power limits and charging profiles that are determined using PBMs and not empirical models.

The ultimate conclusion is that BMS based on ECMs can work well, as demonstrated by millions of existing products. But, they are not optimal. There remains room for improvement.

There have been a number of significant obstacles that have delayed adoption of PBMs in BMS. These include:

- It is more difficult for engineers having traditional educational backgrounds to learn the fundamentals of PBMs than ECMs. We devoted the majority of Vol. I in this series to developing PBM equations, but we needed only one chapter in that volume to develop ECMs. In the end, however, it is our hope that we were able to show that the processes occurring in a lithium-ion cell are fundamentally simple even if the equations appear daunting. The principal mechanism of lithium movement is diffusion, which is a fairly straightforward concept to understand. Lithium tends to move from high-concentration regions to low-concentration re-

gions within the cell unless energy is applied to the cell from an external source that counteracts this natural movement.

- PBMs contain many more parameters than ECMs; values for these parameters must be determined for any physical cell we wish to model and manage. Historically, it has been necessary to disassemble cells and conduct special-purpose experiments to measure the values of the parameters. This requires highly trained scientists and expensive scientific equipment, neither of which are available to many companies wishing to build a BMS. Cell disassembly may also be forbidden by legal agreements made between a company and its cell supplier. Chap. 3 in this volume teaches methods that can be used to estimate PBM parameter values, most of which do not require cell disassembly.
- Solving PBM equations is computationally more demanding than when using ECMs. For example, the continuum-scale models developed in Vol. I comprise a set of four partial-differential equations (PDEs) coupled by a nonlinear algebraic closure term. A direct solution to this model requires multiphysics software that uses finite-element, finite-volume, or finite-difference methods. However, there are numerous ways to simplify the computational requirements of PBMs. We present our preferred method in Chap. 4 of this volume. The final physics-based reduced-order model (ROM) has computational complexity (number of floating-point operations per solution) similar to that of a high-fidelity ECM.
- BMS algorithms based on PBMs have not been proven in practice to the same extent as for ECMs. However, there is increasing evidence in the literature that research teams around the globe focusing on this topic are finding success in lab-scale implementations. We believe that it is only a matter of time before BMS methods based on PBMs attain a level of maturity that allows their use in commercial applications. Chaps. 5 to 8 in this volume share some methods that use PBMs to determine estimates of SOC, SOH, SOP, and optimized charging profiles.

When we published the first two volumes of this series in 2015, we thought that we were almost ready to write this third volume. We believed that we were about 90 % there. It has taken us a few years to realize that the last 10 % of the background research and development is much more difficult than the first 90 %. Now, we feel like we are 99 % of the way there. But it may well be that the remaining 1 % is more difficult than the first 99 %. Rather than delaying this volume any longer, we chose to move forward and share with you what we do know about the subject, hoping that it will inspire many

of you to continue to move the field forward and accelerate the path toward 100 %. We don't pretend that we have the final answer to every question; in fact, we make mention in many chapters of the topics we know that we don't know enough about. We hope this will provide hints to researchers looking for important directions to pursue. That said, all topics presented in this book have been validated at least in simulation; most have undergone preliminary validation in a laboratory setting.

While there remains room to develop this field far beyond where it is now, we do consider the 99 % that we have to offer to be more than sufficient to build prototype PBM-based BMS for test and evaluation and perhaps even commercial BMS for some applications. The methods we present in detail in this volume have been developed exclusively by the research team at the University of Colorado Colorado Springs and, unlike most BMS algorithms based on ECMs, we have purposefully not sought patent protection for these methods. They are open source and we encourage adoption by the community.[4]

[4] We still recommend that the reader perform their own due diligence and search the patent literature; it may well be that other research teams around the globe have patented methods that are essentially the same.

In the remainder of this chapter, we first review some background topics from Vols. I and II upon which this volume builds. We then specifically review the continuum-scale PDEs that form the PDE PBM full-order model (FOM) that we use as a starting point for this volume. Finally, we transform this model into an equivalent mathematical form that will prove to be required later in the book.

1.1 Background topics and a roadmap to this book

The first volume in this series taught how to make sets of equations or *models* that describe how battery cells work, inside and out. The topics are illustrated iconically by the roadmap in Fig. 1.1.

We first studied empirical ECMs, which can describe input/output (current/voltage) behaviors of battery cells quite well. These models can be used by the BMS algorithms presented in Vol. II to estimate SOC, SOH, SOP, and SOE and to inform balancing decisions. We then looked at PBMs, which can additionally describe the internal electrochemical processes occurring in the cell. Different PBMs exist at different length scales. We noted that some research teams develop models that describe battery physics at molecular scales, but we did not discuss those models in detail. We began our in-depth derivation of cell models at the particle scale, where dynamics occurring inside electrode particles and inside the electrolyte are considered separately. These particle-scale models can be highly accurate but are extremely demanding computationally; it is not feasible to simulate more than a handful of particles using desktop computers. So,

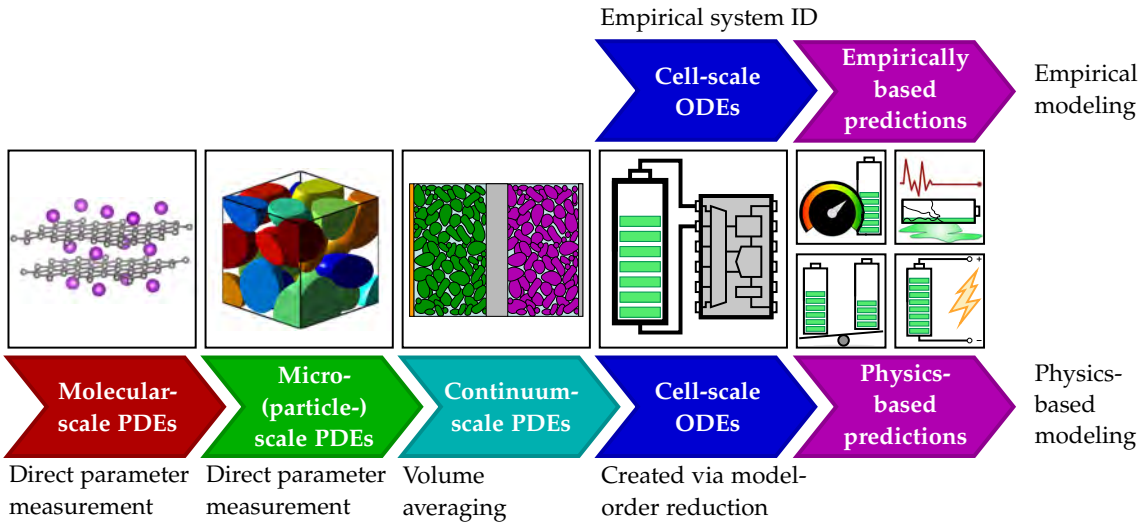

Figure 1.1: Different approaches to making models of lithium-ion cells presented in Vol. I.

we showed how volume-averaging theorems could be applied to the particle-scale equations to produce continuum-scale equations, the Doyle–Fuller–Newman (DFN) pseudo-two-dimensional (P2D) model. This model loses some fidelity by averaging out any existing inhomogeneities in microstructure details, but also greatly reduces the computational complexity of simulating the model—to the point where a desktop computer can often run cell-level simulations in near real time. This P2D model is still not well suited for BMS application, so we proposed the discrete-time realization algorithm (DRA) to approximate the P2D model using a low-order discrete-time state-space model form that has similar computational complexity to a high-fidelity ECM. This ROM is still able to compute predictions of all cell internal electrochemical variables at all spatial locations of interest interior to the cell, in addition to computing predictions of terminal voltage and temperature. This type of model is also suitable for estimating SOC, SOH, SOP, and SOE and to inform balancing decisions, as we will describe later in this volume.

Both kinds of model can be used inside of a BMS to regulate battery-pack usage. The second volume in this series taught how to use ECMs to enable battery-pack controls. The topics covered by that book are illustrated iconically by the roadmap in Fig. 1.2.

Vol. II first gave an overview of BMS requirements and then began to focus on the main algorithm control loop of the BMS. Every measurement interval, battery-pack current, module temperatures, and cell voltages are measured. These are used in combination with a cell model to produce estimates of SOC for all cells in the battery pack. Additional methods were developed to track SOH by updating

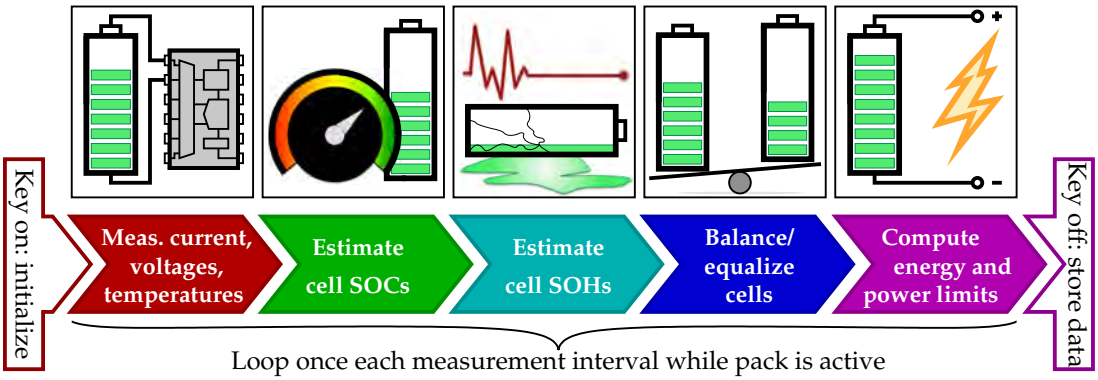

Figure 1.2: The battery-management-system main algorithm control loop presented in Vol. I.

estimates of cell total capacity and resistance as the pack ages. Cell balancing requirements and strategies and power-limits estimation were also covered in detail.

The focus of this third volume is to learn how to perform many of these same tasks, but using PBMs instead of ECMs. To do so, we will need to revisit the modeling and controls aspects of the first two volumes. The first four chapters of this volume are focused on modeling, and the remaining four chapters are focused on controls. The topics of the first four chapters are illustrated iconically by the roadmap figure presented in Fig. 1.3.

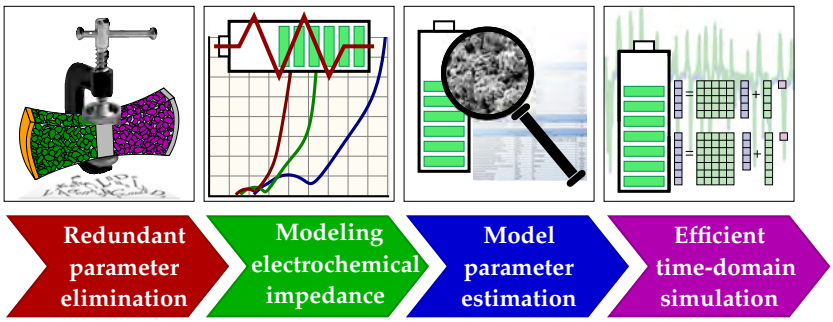

Figure 1.3: Topics in lithium-ion cell modeling that we cover in this volume.

This chapter reviews the continuum-scale DFN P2D model on which this volume is based. It then shows how to reformulate this model to eliminate redundant parameters, which will be necessary when we attempt to estimate the values of these parameters using experimental data. Chap. 2 shows how to enhance the model by adding detail—beyond that considered in the standard DFN model—to equations describing the processes occurring at the electrode/electrolyte interface. It also develops closed-form impedance models of the cell, which can describe frequency-dependent behaviors. Chap. 3 is one of the major contributions of this book, and shows how to estimate values for the parameters of a PBM using input/output

(current/voltage) measurements of the cell in such a way that we frequently do not require cell teardown to characterize a PBM. Only standard types of equipment found in many battery laboratories are needed; specialized training and expensive scientific apparatus are not required. The parameter values determined by the methods of this chapter are used in a full-order PDE-based PBM that is still general; you may choose to adopt any of a number of methods in the literature to simplify this model further for BMS application. However, we present our preferred approach in Chap. 4. It is similar in many ways to the DRA methodology from Vol. I, except that we have shown in Chap. 2 how to improve the transfer functions used as a basis for the method, and we further show how to replace the DRA with a plug-in substitute named the hybrid realization algorithm (HRA), which executes much more quickly and is very robust. We also show how to use the resulting ROM in time-domain simulations across wide cell SOC and temperature operating ranges, and how to simulate constant-voltage and constant-power events.

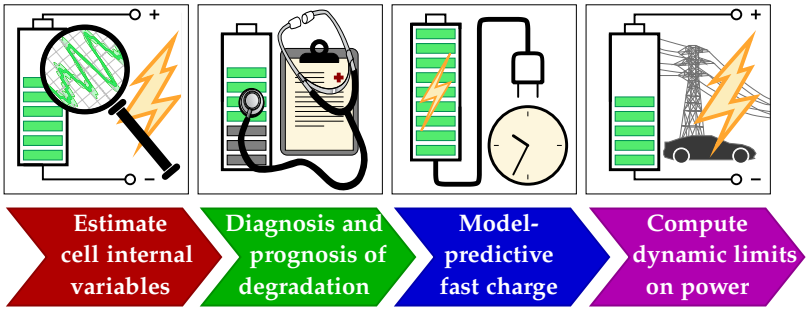

Figure 1.4: Topics in lithium-ion battery control that we cover in this volume.

The topics of the remaining four chapters are illustrated iconically by the roadmap figure presented in Fig. 1.4. Chap. 5 shows how to use the ROM to estimate the entire cell internal electrochemical state, including SOC but far more than that. Chap. 6 considers diagnostics and prognostics applied to aged cells. Chap. 7 teaches how to compute optimal fast-charge profiles using the ROM and a technology known as model-predictive control (MPC). Finally, Chap. 8 shows how to compute power-limit estimates that seek to optimize a trade-off between battery long-term life and short-term performance.

1.2 *Lithium-ion cell models*

In Vol. I, we derived the equations for both ECMs and PBMs. There are advantages and disadvantages to using either inside BMS algorithms. ECMs are tuned by fitting measured current/voltage data to empirical relationships. In operation, the ECM is essentially performing an intelligent interpolation among previously seen data when

using the model to predict the cell voltage at its present operating condition. We need to be cautious when using ECMs: interpolating among measured data can often be done reliably, but extrapolation beyond the measured data is hazardous. An ECM can make good predictions if the present cell operating condition resembles those under which the cell was exercised when collecting data to find the model parameter values. It can make very poor and even nonsensical predictions if the present operating condition is very different from those encountered in the training process. Therefore, large datasets must be collected to train the model and substantial model validation must be performed to ensure that BMS predictions using ECMs are reliable. As we have already mentioned, ECMs are also limited in that they can predict input/output (current/voltage) behaviors only. They cannot predict cell internal electrochemical states. But ECMs have the very positive feature of being numerically robust and computationally simple.

PBMs, on the other hand, tend to have opposite advantages and disadvantages. Unlike ECMs, their equations are based on first principles of electrochemistry and physics and so the models can predict cell behaviors over a wide range of operating conditions, even those not encountered in the laboratory when collecting data to estimate the model parameter values. PBMs also have the ability to predict a cell's internal electrochemical state, which is necessary for aging predictions and for developing fast-charge and power-limits algorithms that consider the impact of cell usage on its rates of degradation. However, traditional PBMs are computationally complex and the PDE solvers required for evaluating their equations are prone to numeric fragility when stimulated using rapidly changing input-current profiles.

Our preferred strategy develops ROMs from the PDEs of the DFN P2D model. These ROMs share all the advantages of both ECMs and PBMs and none of the disadvantages. That is, they can make high-fidelity predictions across a wide range of operating conditions, can predict values for all cell internal electrochemical variables, and have computational complexity similar to a high-accuracy ECM while also maintaining the numeric robustness of an ECM.

In this book, we do not redevelop ECMs or BMS algorithms based on ECMs. Instead, our focus is on using PBMs in BMS algorithms. So, we begin by reviewing the DFN P2D model upon which we base everything that follows.

1.3 *Review of DFN model*

Fig. 1.5 illustrates the geometry of a 1D slice through a lithium-ion cell, roughly to typical scale. The cell comprises three main sections: the negative-electrode, the separator, and the positive-electrode regions.[5] The electrodes themselves are not homogeneous blocks of material; instead, they comprise millions of microscopic particles, increasing the surface area of the electrode/electrolyte interface where the chemical reactions occur. In so doing, this has the effect of decreasing cell resistance and increasing its power capabilities. The figure shows the negative electrode in a green color and the positive electrode in a magenta color for illustrative purposes only; the actual materials are powders that tend to be gray or black in color.

[5] In the literature, the negative electrode is often called the anode and the positive electrode is often called the cathode. Strictly speaking, this terminology is correct only during discharge and must actually be reversed when describing a cell being charged. For this reason, we prefer to use the terms negative and positive electrode instead, to reduce confusion.

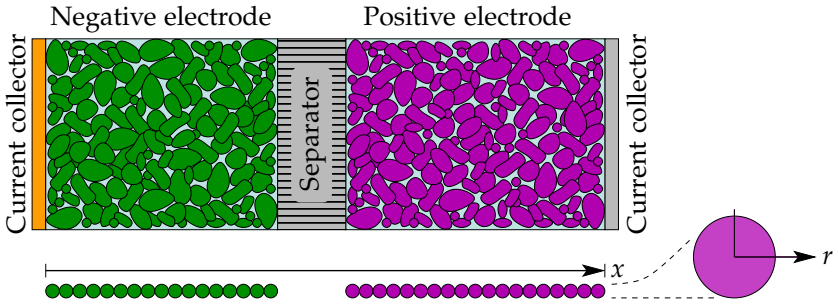

Figure 1.5: Illustration of the cross-sectional geometry of a lithium-ion cell.

The electrode particles are adhered to current collectors, which conduct electronic current to the cell's terminals. Negative-electrode current collectors are made from copper foils and positive-electrode current collectors are made from aluminum foils. The separator is a porous membrane that allows ions to pass through but blocks electron current, preventing the cell from having an internal short circuit. The voids between particles and in the porous separator are permeated with an electrolyte, which conducts ions from one cell region to another but is insulating to electron flow.

In the diagram, the thickness dimension is denoted by the variable x. The P2D model simplifies electrode-model equations by assuming that all electrode particles are spherical and have identical radius R_s. Then, the radial dimension inside any particle is denoted by the variable r. In the model, the length dimension is physical but the radial dimension is somewhat artificial because of this assumption: this is why the model is referred to as a "pseudo" two-dimensional model. The radial dimension is the pseudo dimension.

The P2D model describes the operation of a lithium-ion cell using four PDEs along with associated boundary conditions and initial values, as well as a single nonlinear algebraic equation that serves as

a coupling closure term. This set of equations describes the following electrochemical variables of the cell at spatial location x and time t:

- The concentration of lithium in the solid electrode particles, denoted as $c_s(x, r, t)$, and particularly the concentration at the surface of the solid at the boundary between the solid and the electrolyte, denoted as $c_{s,e}(x, t)$;
- The concentration of lithium in the electrolyte, denoted as $c_e(x, t)$;
- The potential in the solid electrode particles, denoted as $\phi_s(x, t)$;
- The potential in the electrolyte, denoted as $\phi_e(x, t)$;
- The lithium flux (rate of lithium movement between solid electrode particles and the electrolyte), denoted as $j(x, t)$.

We now review the model equations. In the following, note that all variables are functions of x and t, but this dependence will be dropped from the notation unless it is required to clarify some specific point. Further, all parameters are functions of the cell region being described by the equation being reviewed, but their values are assumed to be uniform (constant) across that cell region.

EQUATION 1: Charge conservation in the solid.

The first equation we review describes charge conservation within the solid particles that form an electrode. This is modeled as:[6]

$$\frac{\partial}{\partial x}\sigma^{r}_{eff}\frac{\partial}{\partial x}\phi^{r}_{s} = a^{r}_{s}Fj^{r}, \tag{1.1}$$

where σ^{r}_{eff} is the effective conductivity of the electrode, a^{r}_{s} is the specific interfacial surface area of the electrode, and F is Faraday's constant.[7] This equation applies only to the negative-electrode and positive-electrode regions of the cell. It is a linear diffusion equation describing electron movement, with a forcing term that models flux of electrons, which is equal to the flux of lithium from the electrode to the electrolyte locally.

The boundary conditions for the PDE can be stated as:

$$\sigma^{n}_{eff}\frac{\partial}{\partial x}\phi^{n}_{s}\bigg|_{x=0} = \sigma^{p}_{eff}\frac{\partial}{\partial x}\phi^{p}_{s}\bigg|_{x=L^{tot}} = \frac{-i_{app}}{A}, \tag{1.2}$$

$$\frac{\partial}{\partial x}\phi^{n}_{s}\bigg|_{x=L^{n}} = \frac{\partial}{\partial x}\phi^{p}_{s}\bigg|_{x=L^{n}+L^{s}} = 0, \tag{1.3}$$

where L^n is the thickness of the negative electrode, L^s is the thickness of the separator, L^p is the thickness of the positive electrode, $L^{tot} = L^n + L^s + L^p$, A is the surface area of the current collector, and i_{app} is the electrical current measured at the terminals of the cell.[8]

The initial values for this PDE are:

$$\phi^{n}_{s,0} = 0, \quad \text{and} \quad \phi^{p}_{s,0} = U^{p}_{ocp}(\theta^{p}_{s,0}) - U^{n}_{ocp}(\theta^{n}_{s,0}), \tag{1.4}$$

[6] An appendix to this chapter, Sect. 1.A.2, presents a list defining the parameters of the DFN model for reference.

[7] The superscript "r" for "region" indicates that this equation is parameterized by different constants in different regions of the cell. When it is important to be more specific, we use superscripts "n" for the negative-electrode region, "s" for the separator region, and "p" for the positive-electrode region.

[8] In the sign convention that we use in this series of books, $i_{app} > 0$ for discharge currents and $i_{app} < 0$ for charge currents.

where $\theta_s^r = c_s^r / c_{s,max}^r$ is the stoichiometry of the electrode such that $0 \leq \theta_s^r \leq 1$, $\theta_{s,0}^r = c_{s,0}^r / c_{s,max}^r$ is the initial equilibrium stoichiometry of the electrode, and $U_{ocp}^r(\theta_s^r)$ is the open-circuit potential (OCP) of the electrode as a function of local stoichiometry.

EQUATION II: Mass conservation in the solid.

The second PDE describes mass conservation in the solid electrode materials. It is also valid only for the negative-electrode and positive-electrode regions and is modeled as:

$$\frac{\partial c_s^r}{\partial t} = \frac{1}{r^2}\frac{\partial}{\partial r}\left(D_s^r r^2 \frac{\partial c_s^r}{\partial r}\right), \tag{1.5}$$

where D_s^r is the solid diffusivity of the electrode.[9] This equation is a restatement of Fick's second law, formulated in spherical coordinates and assuming spherical symmetry. That is, lithium motion inside electrode particles is modeled as standard linear diffusion.

[9] For now, it is sufficient to think about D_s^r as being constant. However, this diffusivity is truly concentration-dependent. We incorporate a description of this dependence into the model in later chapters.

The boundary conditions imposed on this PDE are:

$$D_s^r \frac{\partial c_s^r}{\partial r}\bigg|_{r=R_s^r} = -j^r, \quad \text{and} \quad D_s^r \frac{\partial c_s^r}{\partial r}\bigg|_{r=0} = 0. \tag{1.6}$$

The initial values are:

$$c_{s,0}^r = c_{s,max}^r \left(\theta_0^r + z_0(\theta_{100}^r - \theta_0^r)\right), \tag{1.7}$$

where $0 \leq z_0 \leq 1$ is initial cell SOC, θ_0^r is the value of θ_s^r when the cell is resting at 0 % SOC, and θ_{100}^r is the value of θ_s^r when the cell is resting at 100 % SOC.

EQUATION III: Charge conservation in the electrolyte.

The third PDE describes charge conservation in the electrolyte and is valid for all cell regions. It is modeled as:

$$\frac{\partial}{\partial x}\kappa_{eff}^r \left(\frac{\partial}{\partial x}\phi_e^r + \frac{2RT\left(t_+^0 - 1\right)}{F}\left(1 + \frac{\partial \ln f_\pm}{\partial \ln c_e}\right)\frac{\partial \ln c_e^r}{\partial x}\right) + a_s^r F j^r = 0, \tag{1.8}$$

where κ_{eff}^r is the effective conductivity of the electrolyte, R is the universal gas constant, t_+^0 is the transference number of the positive ion in the electrolyte with respect to the solvent, and $f_\pm$ is the mean molar activity coefficient.[10] This equation is dominated by linear-diffusion terms, but the $\partial \ln c_e / \partial x$ term modifies the relationship somewhat to account for a nonlinear concentration dependence.

[10] We do not use the region superscript "r" on t_+^0 or on $\partial \ln f_\pm / \partial \ln c_e$ since these relationships are electrolyte properties that we assume to be constant over all regions.

The boundary conditions for this equation enforce the physical constraint that all current at the current-collector boundaries must be electronic and all current at the separator boundaries must be ionic:

$$-\kappa_{eff}^r \left[\frac{\partial}{\partial x}\phi_e^r + \frac{2RT\left(t_+^0 - 1\right)}{F}\left(1 + \frac{\partial \ln f_\pm}{\partial \ln c_e}\right)\frac{\partial \ln c_e^r}{\partial x}\right|_{\substack{x=0 \\ x=L^{tot}}} = 0 \tag{1.9}$$

$$-\kappa^{\mathrm{r}}_{\mathrm{eff}}\left[\frac{\partial}{\partial x}\phi^{\mathrm{r}}_{\mathrm{e}}+\frac{2RT\left(t^0_+-1\right)}{F}\left(1+\frac{\partial \ln f_{\pm}}{\partial \ln c_{\mathrm{e}}}\right)\frac{\partial \ln c^{\mathrm{r}}_{\mathrm{e}}}{\partial x}\right|_{\substack{x=L^{\mathrm{n}}\\ x=L^{\mathrm{n}}+L^{\mathrm{s}}}}=\frac{i_{\mathrm{app}}}{A}. \tag{1.10}$$

Initial values across the entire cell are:[11]

$$\phi^{\mathrm{r}}_{\mathrm{e},0}=-U^{\mathrm{n}}_{\mathrm{ocp}}(\theta^{\mathrm{n}}_{\mathrm{s},0}). \tag{1.11}$$

[11] To see this, notice from Eq. (1.21) that when the cell is in equilibrium, $\phi^{\mathrm{n}}_{\mathrm{s},0}-\phi^{\mathrm{n}}_{\mathrm{e},0}=U^{\mathrm{n}}_{\mathrm{ocp}}(\theta^{\mathrm{n}}_{\mathrm{s},0})$. Further, from Eq. (1.4) we know that $\phi^{\mathrm{n}}_{\mathrm{s},0}=0$ and since the cell is in equilibrium, Eq. (1.10) implies that $\nabla\phi^{\mathrm{r}}_{\mathrm{e}}=0$. Therefore, $\phi^{\mathrm{n}}_{\mathrm{e},0}=\phi^{\mathrm{p}}_{\mathrm{e},0}=-U^{\mathrm{n}}_{\mathrm{ocp}}(\theta^{\mathrm{n}}_{\mathrm{s},0})$.

EQUATION IV: Mass conservation in the electrolyte.

The fourth PDE describes mass conservation in the electrolyte and is valid for all cell regions. It is modeled as:

$$\frac{\partial(\varepsilon^{\mathrm{r}}_{\mathrm{e}}c^{\mathrm{r}}_{\mathrm{e}})}{\partial t}=\frac{\partial}{\partial x}D^{\mathrm{r}}_{\mathrm{e,eff}}\frac{\partial}{\partial x}c^{\mathrm{r}}_{\mathrm{e}}+a^{\mathrm{r}}_{\mathrm{s}}(1-t^0_+)j^{\mathrm{r}}, \tag{1.12}$$

where $\varepsilon^{\mathrm{r}}_{\mathrm{e}}$ is the porosity (volume fraction of the electrolyte in the cell region), and $D^{\mathrm{r}}_{\mathrm{e,eff}}$ is the diffusivity of lithium in the electrolyte. This is again a linear diffusion equation with a forcing term that describes the addition of lithium due to flux of lithium from the electrode into the electrolyte locally. It applies to all regions of the cell.

The boundary conditions for this equation enforce continuity of both electrolyte concentration and flux of lithium across regions of the cell, and also enforce that there be no movement of lithium from inside the cell to the exterior of the cell:

$$\left.\frac{\partial c^{\mathrm{n}}_{\mathrm{e}}}{\partial x}\right|_{x=0}=\left.\frac{\partial c^{\mathrm{p}}_{\mathrm{e}}}{\partial x}\right|_{x=L^{\mathrm{tot}}}=0 \tag{1.13}$$

$$\left.D^{\mathrm{n}}_{\mathrm{e,eff}}\frac{\partial c^{\mathrm{n}}_{\mathrm{e}}}{\partial x}\right|_{x=(L^{\mathrm{n}})^-}=\left.D^{\mathrm{s}}_{\mathrm{e,eff}}\frac{\partial c^{\mathrm{s}}_{\mathrm{e}}}{\partial x}\right|_{x=(L^{\mathrm{n}})^+} \tag{1.14}$$

$$\left.D^{\mathrm{s}}_{\mathrm{e,eff}}\frac{\partial c^{\mathrm{s}}_{\mathrm{e}}}{\partial x}\right|_{x=(L^{\mathrm{n}}+L^{\mathrm{s}})^-}=\left.D^{\mathrm{p}}_{\mathrm{e,eff}}\frac{\partial c^{\mathrm{p}}_{\mathrm{e}}}{\partial x}\right|_{x=(L^{\mathrm{n}}+L^{\mathrm{s}})^+} \tag{1.15}$$

$$\left.c^{\mathrm{n}}_{\mathrm{e}}\right|_{x=(L^{\mathrm{n}})^-}=\left.c^{\mathrm{s}}_{\mathrm{e}}\right|_{x=(L^{\mathrm{n}})^+} \tag{1.16}$$

$$\left.c^{\mathrm{s}}_{\mathrm{e}}\right|_{x=(L^{\mathrm{n}}+L^{\mathrm{s}})^-}=\left.c^{\mathrm{p}}_{\mathrm{e}}\right|_{x=(L^{\mathrm{n}}+L^{\mathrm{s}})^+}. \tag{1.17}$$

Initial values across the cell are:

$$c_{\mathrm{e}}=c_{\mathrm{e},0}. \tag{1.18}$$

EQUATION V: Kinetics.

The final model equation is a nonlinear algebraic closure term known as the Butler–Volmer equation. It describes the kinetics of the cell—the rate of reaction and hence the rate of lithium flux from the electrode particles into the electrolyte:

$$j^{\mathrm{r}}=j^{\mathrm{r}}_0\left\{\exp\left(\frac{(1-\alpha^{\mathrm{r}})F}{RT}\eta^{\mathrm{r}}\right)-\exp\left(\frac{-\alpha^{\mathrm{r}}F}{RT}\eta^{\mathrm{r}}\right)\right\} \tag{1.19}$$

$$j_0^{\mathrm{r}} = k_{\mathrm{norm},0}^{\mathrm{r}} \left(\frac{c_{\mathrm{e}}^{\mathrm{r}}}{c_{\mathrm{e},0}^{\mathrm{r}}} \right)^{1-\alpha^{\mathrm{r}}} \left(1 - \frac{c_{\mathrm{s,e}}^{\mathrm{r}}}{c_{\mathrm{s,max}}^{\mathrm{r}}} \right)^{1-\alpha^{\mathrm{r}}} \left(\frac{c_{\mathrm{s,e}}^{\mathrm{r}}}{c_{\mathrm{s,max}}^{\mathrm{r}}} \right)^{\alpha^{\mathrm{r}}} \tag{1.20}$$

$$\eta^{\mathrm{r}} = \phi_{\mathrm{s}}^{\mathrm{r}} - \phi_{\mathrm{e}}^{\mathrm{r}} - U_{\mathrm{ocp}}^{\mathrm{r}}(c_{\mathrm{s,e}}^{\mathrm{r}}/c_{\mathrm{s,max}}^{\mathrm{r}}) - FR_{\mathrm{f}}^{\mathrm{r}} j^{\mathrm{r}}, \tag{1.21}$$

where α^{r} is the charge-transfer coefficient, η^{r} is the local overpotential, j_0^{r} is the exchange-flux density, $k_{\mathrm{norm},0}^{\mathrm{r}}$ is a reaction-rate constant, and $R_{\mathrm{f}}^{\mathrm{r}}$ is the resistivity of the surface film that may exist on the electrode particles. This equation is valid for the negative- and positive-electrode regions and is a good description of reaction kinetics for constant-current events, but misses some critical cell behaviors at high frequencies. In Chap. 2, we will revisit this kinetics model and enhance it to describe more detail at the interface between the solid and electrolyte that will be important when modeling cell response to dynamic current inputs, especially at high frequencies.

1.4 *Reducing number of parameters: method*

The governing equations listed in Sect. 1.3 contain 36 parameter values (plus $U_{\mathrm{ocp}}^{\mathrm{r}}$ relationships) that must be determined to use the cell model.[12] These are listed in Table 1.1 and summarized in Sect. 1.A.2. If possible, we would like to find ways to estimate the values of these parameters for a specific cell without opening (or tearing down) the cell and performing invasive measurements. That is, we would prefer to use only input/output current/voltage measurements to find parameter values, which is the topic of Chap. 3.

It turns out that some of the parameters in Table 1.1 cannot be estimated uniquely from input/output data. It is mathematically impossible to do so. Technically, we state that these parameters are *nonidentifiable*. However, the governing equations listed in Sect. 1.3 can be manipulated to combine together the nonidentifiable parameters into a smaller group of *lumped parameters* that are possible to estimate from input/output data, at least in principle. The resulting lumped-parameter model (LPM) retains the ability to predict voltage and (scaled) versions of the cell's internal variables, and can be used in BMS algorithms to optimize a tradeoff between performance and life.

The principal new contribution of this chapter is to demonstrate the process for taking the standard PBM equations and converting them to an LPM. This will be required by the parameter-estimation procedures developed in Chap. 3 and will factor into the model enhancements presented in Chap. 2. We will develop the LPM by modifying the standard PBM equation by equation. First, we normalize length scales and then we define new scaled variables to replace the original variables. By the end of this chapter, we will have reformu-

[12] The content of this section has been adapted from: Gregory L. Plett and M. Scott Trimboli, "Process for lumping parameters to enable nondestructive parameter estimation for lithium-ion physics-based models," in *Proceedings of the 35th International Electric Vehicle Symposium and Exhibition (EVS35)*, Oslo, Norway, June 2022.

Table 1.1: Parameters in the standard DFN model.

Negative electrode	Separator	Positive electrode
$\sigma_{\mathrm{eff}}^{\mathrm{n}}$		$\sigma_{\mathrm{eff}}^{\mathrm{p}}$
$a_{\mathrm{s}}^{\mathrm{n}}$		$a_{\mathrm{s}}^{\mathrm{p}}$
L^{n}	L^{s}	L^{p}
$\kappa_{\mathrm{eff}}^{\mathrm{n}}$	$\kappa_{\mathrm{eff}}^{\mathrm{s}}$	$\kappa_{\mathrm{eff}}^{\mathrm{p}}$
$D_{\mathrm{s}}^{\mathrm{n}}$		$D_{\mathrm{s}}^{\mathrm{p}}$
$R_{\mathrm{s}}^{\mathrm{n}}$		$R_{\mathrm{s}}^{\mathrm{p}}$
$\varepsilon_{\mathrm{e}}^{\mathrm{n}}$	$\varepsilon_{\mathrm{e}}^{\mathrm{s}}$	$\varepsilon_{\mathrm{e}}^{\mathrm{p}}$
$D_{\mathrm{e,eff}}^{\mathrm{n}}$	$D_{\mathrm{e,eff}}^{\mathrm{s}}$	$D_{\mathrm{e,eff}}^{\mathrm{p}}$
$k_{\mathrm{norm},0}^{\mathrm{n}}$		$k_{\mathrm{norm},0}^{\mathrm{p}}$
$c_{\mathrm{s,max}}^{\mathrm{n}}$		$c_{\mathrm{s,max}}^{\mathrm{p}}$
α^{n}		α^{p}
$R_{\mathrm{f}}^{\mathrm{n}}$		$R_{\mathrm{f}}^{\mathrm{p}}$
θ_0^{n}		θ_0^{p}
$\theta_{100}^{\mathrm{n}}$		$\theta_{100}^{\mathrm{p}}$
A, t_+^0, $\partial \ln f_\pm / \partial \ln c_{\mathrm{e}}$, $c_{\mathrm{e},0}$ span all		

lated all equations to eliminate redundant parameters, condensing the parameters we must determine from cell tests to characterize the dynamics of a cell to a minimum identifiable set.

1.4.1 Intensive versus extensive quantities

A quick example might help illustrate the issue we are trying to solve. Consider Newton's second law, which states: "force equals mass times acceleration." But this is equivalent to saying, "force equals density times volume times acceleration." So, both $F = ma$ and $F = \rho V a$ are true.

Suppose that we measure $F = 1\,\mathrm{N}$ and $a = 1\,\mathrm{m\,s^{-2}}$. We can easily calculate that $m = F/a = 1\,\mathrm{kg}$. However, based only on these measured F and a, we have *no idea* what are the distinct values of ρ and V.

- We could have $\rho = 1\,\mathrm{kg\,m^{-3}}$ and $V = 1\,\mathrm{m^3}$;
- We could have $\rho = 0.5\,\mathrm{kg\,m^{-3}}$ and $V = 2\,\mathrm{m^3}$;
- We could have $\rho = 2\,\mathrm{kg\,m^{-3}}$ and $V = 0.5\,\mathrm{m^3}$;

and infinitely many other combinations.

The issue is that ρ and V are joined together in Newton's model in a way that is *impossible* to separate mathematically using measurements of only $\{F, a\}$. It simply cannot be done. We would need to perform an independent *kind* of experiment (e.g., measure ρ or V directly) to determine both values with certainty.

Why do we have this problem with our PBMs? Recall from Vol. I that we say that a property is *intensive* if it is a normalized quantity. If everything (dimensions, moles, etc.) in a system is doubled, the value of an intensive property remains unchanged. Examples of intensive properties are pressure, temperature, concentration, and density. Alternately, we say that a property is *extensive* if it is a total quantity. If everything in a system is doubled, the value of an extensive property also doubles. Examples of extensive properties are internal energy, Gibbs free energy, volume, and mass.

In Vol. I we preferred to work with intensive properties. This allowed us to derive models that apply directly to any scale, whereby we scale intensive values to fit a particular application. But, for the parameter-estimation problem that we address in Chap. 3 of this volume, we *require* extensive properties! This is for the same reason that we could compute mass (extensive) in Newton's example but we could not find density (intensive, scaled by volume to compute mass).

So, we will now reformulate the physics-based-model PDEs to lump together groups of parameters that always appear together in

equations and *cannot* be identified independently (although many researchers who do not recognize this problem have tried!). This is like lumping ρ and V by defining a new variable $m = \rho V$. The lumped parameters of the reformulated PBM are identifiable from input/output measurements, whereas the original parameters are not independently identifiable. In the majority of the cases, the effect of the reformulation is simply to convert intensive properties to extensive properties, but there are a few exceptions where more parameters combine to form a group.

1.4.2 *How are we going to do this?*

Before applying the method we will use to the P2D model, we will use it with a simple example to illustrate the process. Assume that we have pairs of measurements (x, y) where $0 \leq x \leq 1$. A possible dataset of such measurements is plotted in Fig. 1.6. For simplicity, we skip the step of normalizing x since it already has a normalized range.

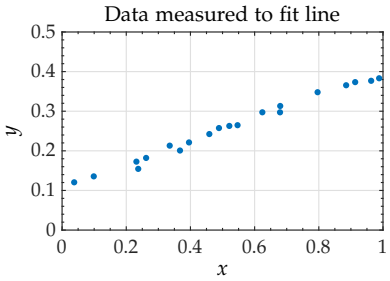

Figure 1.6: Noisy data to which we desire to fit a line.

Now suppose that we desire to fit these data to some physically derived relationship:

$$My = (A + B)x + C. \tag{1.22}$$

We define scaled versions of all of the variables in the equation: we let $\breve{y} = y/\bar{y}$ and $\breve{x} = x/\bar{x}$. In this notation, an overline $(\bar{\cdot})$ indicates a constant (not yet determined)—usually chosen to normalize the primary variable to make the $(\breve{\cdot})$ variable unitless—and $(\breve{\cdot})$ is a temporary notation that indicates a (possibly time-varying) variable that has been normalized and (often) made unitless.

When we make this substitution, we write

$$\begin{aligned} M\bar{y}\breve{y} &= (A + B)\bar{x}\breve{x} + C \\ \breve{y} &= \left[\frac{(A + B)\bar{x}}{M\bar{y}}\right]\breve{x} + \left[\frac{C}{M\bar{y}}\right]. \end{aligned}$$

Now let's look in more detail at the quantities in brackets. We choose to define $\bar{y} = C/M$ and $\bar{x} = C/(A + B)$. Then we have reformulated the original equation to a simpler form,

$$\breve{y} = \breve{x} + 1. \tag{1.23}$$

This equation itself has no more constants that can be estimated.

To implement the physical relationship, we must estimate two quantities from our measured (x, y) data: a modified slope (reciprocal) $\bar{x}$ and a modified y-intercept $\bar{y}$. These two parameters (or variations on these) are the only ones that can be estimated from input/output data. In terms of the original relationship of Eq. (1.22),

it is impossible to find unique values for the parameters A, B, C, and M from input/output data to characterize this model. However, we can implement Eq. (1.23) and solve for $y = \check{y}\bar{y}$ and for $x = \check{x}\bar{x}$ to find the same variables. We have not lost any ability to predict the variables of the model—we have simply lumped constant parameter values together to make it possible to determine the coefficients of the equation via measured data.

1.5 *Reducing number of parameters: application*

We now apply this method to the PBM PDE model, equation by equation, starting with ϕ_s.

EQUATION 1: Charge conservation in solid.

The first step to applying the method is to normalize the cell's 1D thickness dimension by defining:

$$\tilde{x} = (x - x_0^r)/L^r + x_1^r,$$

where x_0^r is the starting location of each region and x_1^r is the index of each region.[13] The result of this normalization is:

$$0 \leq \tilde{x} \leq 1 \text{ in the negative electrode;}$$
$$1 \leq \tilde{x} \leq 2 \text{ in the separator region;}$$
$$2 \leq \tilde{x} \leq 3 \text{ in the positive electrode.}$$

[13] Note that x_0^r is a dimension in meters and x_1^r is a dimensionless zero-based index: $x_1^n = 0$, $x_1^s = 1$, and $x_1^p = 2$.

Then we can also relate derivatives with respect to x to derivatives with respect to $\tilde{x}$:

$$\frac{\partial(\cdot)}{\partial x} = \frac{1}{L^r}\frac{\partial(\cdot)}{\partial \tilde{x}}.$$

The second step to applying the method is to define scaled versions of all variables. For the charge-conservation equation, we let $\check{\phi}_s = \phi_s/\bar{\phi}_s$ and $\check{j} = j/\bar{j}$. Note that this also implies that $\partial\phi_s/\partial(\cdot) = \bar{\phi}_s\partial\check{\phi}_s/\partial(\cdot)$. So, starting with Eq. (1.1), we can write:

$$\frac{\partial}{\partial x}\sigma_{\text{eff}}^r\frac{\partial}{\partial x}\phi_s^r = a_s^r F j^r,$$
$$\frac{\bar{\phi}_s^r\sigma_{\text{eff}}^r}{(L^r)^2}\frac{\partial^2}{\partial \tilde{x}^2}\check{\phi}_s^r = a_s^r F \bar{j}^r \check{j}^r$$
$$\frac{\partial^2}{\partial \tilde{x}^2}\check{\phi}_s^r = F\left[\frac{a_s^r(L^r)^2\bar{j}^r}{\bar{\phi}_s^r\sigma_{\text{eff}}^r}\right]\check{j}^r.$$

We will ultimately define $\bar{j}^r$ and $\bar{\phi}_s^r$ to make the bracketed constant in this equation disappear, to help minimize the number of parameter values that must be determined.

Using the same approach, the nonzero boundary conditions of Eq. (1.2) are rewritten as:

$$\frac{\sigma^{\mathrm{n}}_{\mathrm{eff}}\bar{\phi}^{\mathrm{n}}_{\mathrm{s}}}{L^{\mathrm{n}}}\frac{\partial}{\partial\tilde{x}}\breve{\phi}^{\mathrm{n}}_{\mathrm{s}}\bigg|_{\tilde{x}=0} = \frac{\sigma^{\mathrm{p}}_{\mathrm{eff}}\bar{\phi}^{\mathrm{p}}_{\mathrm{s}}}{L^{\mathrm{p}}}\frac{\partial}{\partial\tilde{x}}\breve{\phi}^{\mathrm{p}}_{\mathrm{s}}\bigg|_{\tilde{x}=3} = \frac{-i_{\mathrm{app}}}{A}$$

$$\left[\frac{A\sigma^{\mathrm{n}}_{\mathrm{eff}}\bar{\phi}^{\mathrm{n}}_{\mathrm{s}}}{L^{\mathrm{n}}}\right]\frac{\partial}{\partial\tilde{x}}\breve{\phi}^{\mathrm{n}}_{\mathrm{s}}\bigg|_{\tilde{x}=0} = \left[\frac{A\sigma^{\mathrm{p}}_{\mathrm{eff}}\bar{\phi}^{\mathrm{p}}_{\mathrm{s}}}{L^{\mathrm{p}}}\right]\frac{\partial}{\partial\tilde{x}}\breve{\phi}^{\mathrm{p}}_{\mathrm{s}}\bigg|_{\tilde{x}=3} = -i_{\mathrm{app}}.$$

Finally, we consider the initial values from Eq. (1.4):

- $\phi^{\mathrm{n}}_{\mathrm{s},0} = \breve{\phi}^{\mathrm{n}}_{\mathrm{s}} = 0$ in the negative electrode.
- $\phi^{\mathrm{p}}_{\mathrm{s},0} = U^{\mathrm{p}}_{\mathrm{ocp}}(\theta^{\mathrm{p}}_{\mathrm{s},0}) - U^{\mathrm{n}}_{\mathrm{ocp}}(\theta^{\mathrm{n}}_{\mathrm{s},0})$ in the positive electrode so,

$$\breve{\phi}^{\mathrm{p}}_{\mathrm{s},0} = \left(U^{\mathrm{p}}_{\mathrm{ocp}}(\theta^{\mathrm{p}}_{\mathrm{s},0}) - U^{\mathrm{n}}_{\mathrm{ocp}}(\theta^{\mathrm{n}}_{\mathrm{s},0})\right)/\bar{\phi}^{\mathrm{p}}_{\mathrm{s}}.$$

The third step to applying the method is to make assignments to the scaling constants to simplify the equations. We choose to:

- Let $\bar{\phi}^{\mathrm{r}}_{\mathrm{s}} = \frac{L^{\mathrm{r}}}{A\sigma^{\mathrm{r}}_{\mathrm{eff}}}$ and define $\bar{\sigma}^{\mathrm{r}} = \frac{A\sigma^{\mathrm{r}}_{\mathrm{eff}}}{L^{\mathrm{r}}}$,[14] so $\bar{\phi}^{\mathrm{r}}_{\mathrm{s}} = 1/\bar{\sigma}^{\mathrm{r}}$.[15]
- Let $\bar{j}^{\mathrm{r}} = \frac{1}{a^{\mathrm{r}}_{\mathrm{s}}AL^{\mathrm{r}}}$.

[14] The original parameter $\sigma^{\mathrm{r}}_{\mathrm{eff}}$ is the *intensive* effective solid conductivity of region r in [S m^{-1}] whereas the lumped parameter $\bar{\sigma}^{\mathrm{r}}$ is the *extensive* effective solid conductivity of region r in [S].

[15] Notice that the constant $\bar{\phi}^{\mathrm{r}}_{\mathrm{s}}$ has units of [Ω] and not [V]; in the procedure that we use, over-bar quantities do not need to have the same units as the variables that they normalize.

This reduces the PDE, its boundary conditions, and initial values to:

$$\begin{aligned}
\frac{\partial^2\breve{\phi}^{\mathrm{r}}_{\mathrm{s}}}{\partial\tilde{x}^2} &= F\breve{j}^{\mathrm{r}} \\
\frac{\partial}{\partial\tilde{x}}\breve{\phi}^{\mathrm{r}}_{\mathrm{s}}\bigg|_{\tilde{x}=0} &= \frac{\partial}{\partial\tilde{x}}\breve{\phi}^{\mathrm{r}}_{\mathrm{s}}\bigg|_{\tilde{x}=3} = -i_{\mathrm{app}} \\
\breve{\phi}^{\mathrm{n}}_{\mathrm{s},0} &= 0 \\
\breve{\phi}^{\mathrm{p}}_{\mathrm{s},0} &= \left(U^{\mathrm{p}}_{\mathrm{ocp}}(\theta^{\mathrm{p}}_{\mathrm{s},0}) - U^{\mathrm{n}}_{\mathrm{ocp}}(\theta^{\mathrm{n}}_{\mathrm{s},0})\right)/\bar{\phi}^{\mathrm{p}}_{\mathrm{s}}.
\end{aligned}$$

This process has completely eliminated all cell-dependent parameters from the PDE and its boundary conditions, but we still must estimate $\bar{\phi}^{\mathrm{p}}_{\mathrm{s}}$ and specify $\theta^{\mathrm{n}}_{\mathrm{s},0}$ and $\theta^{\mathrm{p}}_{\mathrm{s},0}$ to be able to describe initial values. We must also determine the open-circuit-potential relationships $U^{\mathrm{r}}_{\mathrm{ocp}}(\theta^{\mathrm{r}}_{\mathrm{s}})$ for both electrodes.

EQUATION II: Mass conservation in solid.

We now apply the same process to the PDE describing mass conservation in the solid, Eq. (1.5). We normalize the radial pseudo dimension by defining $\tilde{r} = r/R^{\mathrm{r}}_{\mathrm{s}}$; then, $\tilde{r} = 0$ at the center of a particle and $\tilde{r} = 1$ at the surface of a particle. We also define $\breve{c}^{\mathrm{r}}_{\mathrm{s}} = c^{\mathrm{r}}_{\mathrm{s}}/\bar{c}^{\mathrm{r}}_{\mathrm{s}}$.

Substituting these definitions into Eq. (1.5), we can write:

$$\begin{aligned}
\frac{\partial c^{\mathrm{r}}_{\mathrm{s}}}{\partial t} &= \frac{1}{r^2}\frac{\partial}{\partial r}\left(D^{\mathrm{r}}_{\mathrm{s}}r^2\frac{\partial c_{\mathrm{s}}}{\partial r}\right) \\
\bar{c}^{\mathrm{r}}_{\mathrm{s}}\frac{\partial\breve{c}^{\mathrm{r}}_{\mathrm{s}}}{\partial t} &= \frac{1}{(R^{\mathrm{r}}_{\mathrm{s}}\tilde{r})^2}\frac{1}{R^{\mathrm{r}}_{\mathrm{s}}}\frac{\partial}{\partial\tilde{r}}\left(D^{\mathrm{r}}_{\mathrm{s}}(R^{\mathrm{r}}_{\mathrm{s}}\tilde{r})^2\frac{\bar{c}^{\mathrm{r}}_{\mathrm{s}}}{R^{\mathrm{r}}_{\mathrm{s}}}\frac{\partial\breve{c}^{\mathrm{r}}_{\mathrm{s}}}{\partial\tilde{r}}\right) \\
\frac{\partial\breve{c}^{\mathrm{r}}_{\mathrm{s}}}{\partial t} &= \frac{1}{\tilde{r}^2}\frac{\partial}{\partial\tilde{r}}\left(\left[\frac{D^{\mathrm{r}}_{\mathrm{s}}}{(R^{\mathrm{r}}_{\mathrm{s}})^2}\right]\tilde{r}^2\frac{\partial\breve{c}^{\mathrm{r}}_{\mathrm{s}}}{\partial\tilde{r}}\right).
\end{aligned}$$

The nonzero boundary condition of Eq. (1.6) is:

$$\begin{aligned} D_{\mathrm{s}}^{\mathrm{r}} \frac{\partial c_{\mathrm{s}}}{\partial r}\bigg|_{r=R_{\mathrm{s}}^{\mathrm{r}}} &= -j^{\mathrm{r}} \\ \frac{D_{\mathrm{s}}^{\mathrm{r}} \bar{c}_{\mathrm{s}}^{\mathrm{r}}}{R_{\mathrm{s}}^{\mathrm{r}}} \frac{\partial \breve{c}_{\mathrm{s}}^{\mathrm{r}}}{\partial \tilde{r}}\bigg|_{\tilde{r}=1} &= -\bar{j}^{\mathrm{r}} \breve{j}^{\mathrm{r}} \\ \frac{\partial \breve{c}_{\mathrm{s}}^{\mathrm{r}}}{\partial \tilde{r}}\bigg|_{\tilde{r}=1} &= -\left[\frac{\bar{j}^{\mathrm{r}} R_{\mathrm{s}}^{\mathrm{r}}}{D_{\mathrm{s}}^{\mathrm{r}} \bar{c}_{\mathrm{s}}^{\mathrm{r}}}\right] \breve{j}^{\mathrm{r}}. \end{aligned}$$

The initial values of Eq. (1.7) can be rewritten as:

$$\begin{aligned} c_{\mathrm{s},0}^{\mathrm{r}} &= c_{\mathrm{s,max}}^{\mathrm{r}} \left(\theta_0^{\mathrm{r}} + z_0(\theta_{100}^{\mathrm{r}} - \theta_0^{\mathrm{r}})\right) \\ \breve{c}_{\mathrm{s},0}^{\mathrm{r}} &= \bar{c}_{\mathrm{s,max}}^{\mathrm{r}} \left(\theta_0^{\mathrm{r}} + z_0(\theta_{100}^{\mathrm{r}} - \theta_0^{\mathrm{r}})\right). \end{aligned}$$

We now make additional assignments, defining:

- $\bar{D}_{\mathrm{s}}^{\mathrm{r}} = \frac{D_{\mathrm{s}}^{\mathrm{r}}}{(R_{\mathrm{s}}^{\mathrm{r}})^2}$;
- $\bar{c}_{\mathrm{s}}^{\mathrm{r}} = \frac{\bar{j}^{\mathrm{r}} R_{\mathrm{s}}^{\mathrm{r}}}{D_{\mathrm{s}}^{\mathrm{r}}}$ and $\bar{c}_{\mathrm{s,max}}^{\mathrm{r}} = \frac{c_{\mathrm{s,max}}^{\mathrm{r}}}{\bar{c}_{\mathrm{s}}^{\mathrm{r}}} = \frac{a_{\mathrm{s}}^{\mathrm{r}} A L^{\mathrm{r}} c_{\mathrm{s,max}}^{\mathrm{r}} D_{\mathrm{s}}^{\mathrm{r}}}{R_{\mathrm{s}}^{\mathrm{r}}}$.

Note that cell total capacity (in Ah) can be written as:[16,17]

$$Q = \varepsilon_{\mathrm{s}}^{\mathrm{r}} A L^{\mathrm{r}} F c_{\mathrm{s,max}}^{\mathrm{r}} \left|\theta_{100}^{\mathrm{r}} - \theta_0^{\mathrm{r}}\right| / 3600.$$

If we assume that electrode particles are spherical, then $\varepsilon_{\mathrm{s}}^{\mathrm{r}} = a_{\mathrm{s}}^{\mathrm{r}} R_{\mathrm{s}}^{\mathrm{r}}/3$. So,

$$\begin{aligned} Q &= \frac{a_{\mathrm{s}}^{\mathrm{r}} A L^{\mathrm{r}} F c_{\mathrm{s,max}}^{\mathrm{r}} R_{\mathrm{s}}^{\mathrm{r}}}{10\,800} \left|\theta_{100}^{\mathrm{r}} - \theta_0^{\mathrm{r}}\right| \\ &= \frac{\bar{c}_{\mathrm{s,max}}^{\mathrm{r}} F (R_{\mathrm{s}}^{\mathrm{r}})^2}{10\,800 D_{\mathrm{s}}^{\mathrm{r}}} \left|\theta_{100}^{\mathrm{r}} - \theta_0^{\mathrm{r}}\right|, \end{aligned}$$

or

$$\bar{c}_{\mathrm{s,max}}^{\mathrm{r}} = \frac{10\,800 \bar{D}_{\mathrm{s}}^{\mathrm{r}} Q}{F \left|\theta_{100}^{\mathrm{r}} - \theta_0^{\mathrm{r}}\right|}. \tag{1.24}$$

The benefit of this analysis is that we have replaced two unknown constants, $\bar{c}_{\mathrm{s,max}}^{\mathrm{n}}$ and $\bar{c}_{\mathrm{s,max}}^{\mathrm{p}}$, with a single relationship in terms of a single (easily measurable) cell parameter Q and other constants that must be determined in any case when identifying a model of a lithium-ion cell. We can now express the PDE, its nonzero boundary condition, and its initial values as:

$$\begin{aligned} \frac{\partial \breve{c}_{\mathrm{s}}^{\mathrm{r}}}{\partial t} &= \frac{1}{\tilde{r}^2} \frac{\partial}{\partial \tilde{r}} \left(\bar{D}_{\mathrm{s}}^{\mathrm{r}} \tilde{r}^2 \frac{\partial \breve{c}_{\mathrm{s}}^{\mathrm{r}}}{\partial \tilde{r}}\right) \\ \frac{\partial \breve{c}_{\mathrm{s}}^{\mathrm{r}}}{\partial \tilde{r}}\bigg|_{\tilde{r}=1} &= -\breve{j}^{\mathrm{r}} \\ \breve{c}_{\mathrm{s},0}^{\mathrm{r}} &= \frac{10\,800 \bar{D}_{\mathrm{s}}^{\mathrm{r}} Q}{F \left|\theta_{100}^{\mathrm{r}} - \theta_0^{\mathrm{r}}\right|} \left(\theta_0^{\mathrm{r}} + z_0(\theta_{100}^{\mathrm{r}} - \theta_0^{\mathrm{r}})\right). \end{aligned}$$

At this point, the list of unknown parameters that we must estimate comprises: Q, $\bar{\sigma}^{\mathrm{p}}$, θ_0^{n}, θ_0^{p}, $\theta_{100}^{\mathrm{n}}$, $\theta_{100}^{\mathrm{p}}$, $\bar{D}_{\mathrm{s}}^{\mathrm{n}}$, and $\bar{D}_{\mathrm{s}}^{\mathrm{p}}$.

[16] Note that electrochemists may be more comfortable expressing capacity in mol rather than Ah. However, we believe that most engineers will be more familiar with expressing capacity in Ah, and so this will be our convention.

[17] This equation relates cell-level measured total capacity to electrode-level utilized capacity. Each electrode actually has greater theoretical capacity than Q, but the utilized capacity is determined by the width of the stoichiometric operating window defined by θ_0^{r} and $\theta_{100}^{\mathrm{r}}$.

EQUATION III: Charge conservation in the electrolyte.

We proceed by applying the same methodology to the PDE that describes charge conservation in the electrolyte, Eq. (1.8). We let $\breve{\phi}_{\mathrm{e}}^{\mathrm{r}} = \phi_{\mathrm{e}}^{\mathrm{r}}/\bar{\phi}_{\mathrm{e}}^{\mathrm{r}}$ and $\breve{c}_{\mathrm{e}}^{\mathrm{r}} = c_{\mathrm{e}}^{\mathrm{r}}/\bar{c}_{\mathrm{e}}^{\mathrm{r}}$. This gives:

$$\frac{\partial}{\partial x}\kappa_{\mathrm{eff}}^{\mathrm{r}}\left(\frac{\partial}{\partial x}\phi_{\mathrm{e}}^{\mathrm{r}} + \frac{2RT\left(t_+^0-1\right)}{F}\left(1+\frac{\partial \ln f_\pm}{\partial \ln c_{\mathrm{e}}}\right)\frac{\partial \ln c_{\mathrm{e}}^{\mathrm{r}}}{\partial x}\right) + a_{\mathrm{s}}^{\mathrm{r}} F j^{\mathrm{r}} = 0$$

$$\frac{1}{L^{\mathrm{r}}}\frac{\partial}{\partial \tilde{x}}\left(\frac{\kappa_{\mathrm{eff}}^{\mathrm{r}}\bar{\phi}_{\mathrm{e}}^{\mathrm{r}}}{L^{\mathrm{r}}}\frac{\partial}{\partial \tilde{x}}\breve{\phi}_{\mathrm{e}}^{\mathrm{r}} + \frac{\kappa_{\mathrm{eff}}^{\mathrm{r}}}{L^{\mathrm{r}}}\frac{2RT\left(t_+^0-1\right)}{F}\left(1+\frac{\partial \ln f_\pm}{\partial \ln c_{\mathrm{e}}}\right)\frac{\partial \ln \breve{c}_{\mathrm{e}}^{\mathrm{r}}}{\partial \tilde{x}}\right) + a_{\mathrm{s}}^{\mathrm{r}} F \bar{j}^{\mathrm{r}} \breve{j}^{\mathrm{r}} = 0$$

$$\frac{\partial}{\partial \tilde{x}}\left(\left[\frac{\kappa_{\mathrm{eff}}^{\mathrm{r}} A \bar{\phi}_{\mathrm{e}}^{\mathrm{r}}}{L^{\mathrm{r}}}\right]\frac{\partial}{\partial \tilde{x}}\breve{\phi}_{\mathrm{e}}^{\mathrm{r}} + T\left[\frac{2R(t_+^0-1)}{F}\left(1+\frac{\partial \ln f_\pm}{\partial \ln c_{\mathrm{e}}}\right)\frac{\kappa_{\mathrm{eff}}^{\mathrm{r}} A}{L^{\mathrm{r}}}\right]\frac{\partial \ln \breve{c}_{\mathrm{e}}^{\mathrm{r}}}{\partial \tilde{x}}\right) + \underbrace{a_{\mathrm{s}}^{\mathrm{r}} A F L^{\mathrm{r}} \bar{j}^{\mathrm{r}}}_{F}\breve{j}^{\mathrm{r}} = 0.$$

The nonzero boundary conditions from Eq. (1.10) are:

$$-\kappa_{\mathrm{eff}}^{\mathrm{r}}\left[\frac{\partial}{\partial x}\phi_{\mathrm{e}}^{\mathrm{r}} + \frac{2RT\left(t_+^0-1\right)}{F}\left(1+\frac{\partial \ln f_\pm}{\partial \ln c_{\mathrm{e}}}\right)\frac{\partial \ln c_{\mathrm{e}}^{\mathrm{r}}}{\partial x}\right|_{\substack{x=L^{\mathrm{n}} \\ x=L^{\mathrm{n}}+L^{\mathrm{s}}}} = \frac{i_{\mathrm{app}}}{A}$$

$$-\left[\frac{\kappa_{\mathrm{eff}}^{\mathrm{r}} A \bar{\phi}_{\mathrm{e}}^{\mathrm{r}}}{L^{\mathrm{r}}}\right]\frac{\partial}{\partial \tilde{x}}\breve{\phi}_{\mathrm{e}}^{\mathrm{r}} - T\left[\frac{2R(t_+^0-1)}{F}\left(1+\frac{\partial \ln f_\pm}{\partial \ln c_{\mathrm{e}}}\right)\frac{\kappa_{\mathrm{eff}}^{\mathrm{r}} A}{L^{\mathrm{r}}}\right]\frac{\partial \ln \breve{c}_{\mathrm{e}}^{\mathrm{r}}}{\partial \tilde{x}}\right|_{\tilde{x}=1,2} = i_{\mathrm{app}}.$$

The initial values are reformulated from Eq. (1.11) as:

$$\phi_{\mathrm{e},0}^{\mathrm{r}} = -U_{\mathrm{ocp}}^{\mathrm{n}}(\theta_{\mathrm{s},0}^{\mathrm{n}}) \quad \text{and so} \ldots \quad \breve{\phi}_{\mathrm{e},0}^{\mathrm{r}} = -U_{\mathrm{ocp}}^{\mathrm{n}}(\theta_{\mathrm{s},0}^{\mathrm{n}})/\bar{\phi}_{\mathrm{e}}^{\mathrm{r}},$$

where $\theta_{\mathrm{s},0}^{\mathrm{r}} = c_{\mathrm{s},0}^{\mathrm{r}}/c_{\mathrm{s,max}}^{\mathrm{r}}$.

We define:

- $\bar{\phi}_{\mathrm{e}}^{\mathrm{r}} = \frac{L^{\mathrm{r}}}{\kappa_{\mathrm{eff}}^{\mathrm{r}} A}$ and $\bar{\kappa}^{\mathrm{r}} = \frac{A\kappa_{\mathrm{eff}}^{\mathrm{r}}}{L^{\mathrm{r}}}$, so $\bar{\phi}_{\mathrm{e}}^{\mathrm{r}} = 1/\bar{\kappa}^{\mathrm{r}}$;
- $\bar{\kappa}_D = \frac{2R(t_+^0-1)}{F}\left(1 + \frac{\partial \ln f_\pm}{\partial \ln c_{\mathrm{e}}}\right)$.

This reduces the PDE and its nonzero boundary conditions to:

$$\frac{\partial}{\partial \tilde{x}}\left(\frac{\partial}{\partial \tilde{x}}\breve{\phi}_{\mathrm{e}}^{\mathrm{r}} + T\left[\bar{\kappa}_D \bar{\kappa}^{\mathrm{r}}\right]\frac{\partial \ln\left(\breve{c}_{\mathrm{e}}^{\mathrm{r}}\right)}{\partial \tilde{x}}\right) + F\breve{j}^{\mathrm{r}} = 0$$

$$-\frac{\partial}{\partial \tilde{x}}\breve{\phi}_{\mathrm{e}}^{\mathrm{r}} - T\left[\bar{\kappa}_D \bar{\kappa}^{\mathrm{r}}\right]\frac{\partial \ln\left(\breve{c}_{\mathrm{e}}^{\mathrm{r}}\right)}{\partial \tilde{x}}\bigg|_{\tilde{x}=1,2} = i_{\mathrm{app}}.$$

$$\breve{\phi}_{\mathrm{e},0}^{\mathrm{r}} = -U_{\mathrm{ocp}}^{\mathrm{n}}(\theta_{\mathrm{s,e}}^{\mathrm{n}})/\bar{\phi}_{\mathrm{e}}^{\mathrm{r}}.$$

This PDE adds $\bar{\kappa}^{\mathrm{n}}$, $\bar{\kappa}^{\mathrm{s}}$, $\bar{\kappa}^{\mathrm{p}}$, and $\bar{\kappa}_D$ to the list of values that must be identified.

EQUATION IV: Mass conservation in the electrolyte.

We now apply the method to the mass-conservation in electrolyte PDE, Eq. (1.12):

$$\frac{\partial(\varepsilon_{\mathrm{e}}^{\mathrm{r}} c_{\mathrm{e}}^{\mathrm{r}})}{\partial t} = \frac{\partial}{\partial x}D_{\mathrm{e,eff}}^{\mathrm{r}}\frac{\partial}{\partial x}c_{\mathrm{e}}^{\mathrm{r}} + a_{\mathrm{s}}^{\mathrm{r}}(1-t_+^0)j^{\mathrm{r}}$$

$$\varepsilon_{\mathrm{e}}^{\mathrm{r}}\bar{c}_{\mathrm{e}}^{\mathrm{r}}\frac{\partial \breve{c}_{\mathrm{e}}^{\mathrm{r}}}{\partial t} = \frac{1}{L^{\mathrm{r}}}\frac{\partial}{\partial \tilde{x}}\frac{D_{\mathrm{e,eff}}^{\mathrm{r}}\bar{c}_{\mathrm{e}}^{\mathrm{r}}}{L^{\mathrm{r}}}\frac{\partial}{\partial \tilde{x}}\breve{c}_{\mathrm{e}}^{\mathrm{r}} + a_{\mathrm{s}}^{\mathrm{r}}(1-t_{+}^{0})\bar{j}^{\mathrm{r}}\breve{j}^{\mathrm{r}}$$
$$\left[\frac{\varepsilon_{\mathrm{e}}^{\mathrm{r}}\bar{c}_{\mathrm{e}}^{\mathrm{r}}AL^{\mathrm{r}}}{1-t_{+}^{0}}\right]\frac{\partial \breve{c}_{\mathrm{e}}^{\mathrm{r}}}{\partial t} = \frac{\partial}{\partial \tilde{x}}\left[\frac{D_{\mathrm{e,eff}}^{\mathrm{r}}A\bar{c}_{\mathrm{e}}^{\mathrm{r}}}{L^{\mathrm{r}}(1-t_{+}^{0})}\right]\frac{\partial}{\partial \tilde{x}}\breve{c}_{\mathrm{e}}^{\mathrm{r}} + \breve{j}^{\mathrm{r}}.$$

The nonzero slope boundary condition at the negative-electrode/separator interface, Eq. (1.14), is:

$$D_{\mathrm{e,eff}}^{\mathrm{n}}\frac{\partial c_{\mathrm{e}}^{\mathrm{n}}}{\partial x}\bigg|_{x=(L^{\mathrm{n}})^{-}} = D_{\mathrm{e,eff}}^{\mathrm{s}}\frac{\partial c_{\mathrm{e}}^{\mathrm{s}}}{\partial x}\bigg|_{x=(L^{\mathrm{n}})^{+}}$$
$$\left[\frac{D_{\mathrm{e,eff}}^{\mathrm{n}}A\bar{c}_{\mathrm{e}}^{\mathrm{n}}}{L^{\mathrm{n}}(1-t_{+}^{0})}\right]\frac{\partial \breve{c}_{\mathrm{e}}^{\mathrm{n}}}{\partial \tilde{x}}\bigg|_{\tilde{x}=1^{-}} = \left[\frac{D_{\mathrm{e,eff}}^{\mathrm{s}}A\bar{c}_{\mathrm{e}}^{\mathrm{s}}}{L^{\mathrm{s}}(1-t_{+}^{0})}\right]\frac{\partial \breve{c}_{\mathrm{e}}^{\mathrm{s}}}{\partial \tilde{x}}\bigg|_{\tilde{x}=1^{+}}.$$

The nonzero slope boundary condition at the separator/positive-electrode interface, Eq. (1.15), is:

$$\left[\frac{D_{\mathrm{e,eff}}^{\mathrm{s}}A\bar{c}_{\mathrm{e}}^{\mathrm{s}}}{L^{\mathrm{s}}(1-t_{+}^{0})}\right]\frac{\partial \breve{c}_{\mathrm{e}}^{\mathrm{s}}}{\partial \tilde{x}}\bigg|_{\tilde{x}=2^{-}} = \left[\frac{D_{\mathrm{e,eff}}^{\mathrm{p}}A\bar{c}_{\mathrm{e}}^{\mathrm{p}}}{L^{\mathrm{p}}(1-t_{+}^{0})}\right]\frac{\partial \breve{c}_{\mathrm{e}}^{\mathrm{p}}}{\partial \tilde{x}}\bigg|_{\tilde{x}=2^{+}}.$$

The continuity boundary conditions at the electrode/separator boundaries, Eqs. (1.16)–(1.17), are:

$$\breve{c}_{\mathrm{e}}^{\mathrm{n}}|_{\tilde{x}=1^{-}} = \breve{c}_{\mathrm{e}}^{\mathrm{s}}|_{\tilde{x}=1^{+}}$$
$$\breve{c}_{\mathrm{e}}^{\mathrm{s}}|_{\tilde{x}=2^{-}} = \breve{c}_{\mathrm{e}}^{\mathrm{p}}\Big|_{\tilde{x}=2^{+}}.$$

The initial values from Eq. (1.18) are reformulated as:

$$c_{\mathrm{e}}^{\mathrm{r}}(x,0) = c_{\mathrm{e},0}$$
$$\breve{c}_{\mathrm{e}}^{\mathrm{r}}(\tilde{x},0) = \frac{c_{\mathrm{e},0}}{\bar{c}_{\mathrm{e}}^{\mathrm{r}}}.$$

We define $\bar{c}_{\mathrm{e}}^{\mathrm{r}} = c_{\mathrm{e},0}$, which makes $\breve{c}_{\mathrm{e}}^{\mathrm{r}}(\tilde{x},0) = \breve{c}_{\mathrm{e},0}^{\mathrm{r}} = 1$. We further define $\bar{D}_{\mathrm{e}}^{\mathrm{r}} = D_{\mathrm{e,eff}}^{\mathrm{r}}A\bar{c}_{\mathrm{e}}^{\mathrm{r}}/(L^{\mathrm{r}}(1-t_{+}^{0}))$. We temporarily define $\bar{n}_{\mathrm{e}}^{\mathrm{r}} = \varepsilon_{\mathrm{e}}^{\mathrm{r}}\bar{c}_{\mathrm{e}}^{\mathrm{r}}AL^{\mathrm{r}}/(1-t_{+}^{0})$. Then,

$$\bar{n}_{\mathrm{e}}^{\mathrm{r}}\frac{\partial \breve{c}_{\mathrm{e}}^{\mathrm{r}}}{\partial t} = \frac{\partial}{\partial \tilde{x}}\bar{D}_{\mathrm{e}}^{\mathrm{r}}\frac{\partial \breve{c}_{\mathrm{e}}^{\mathrm{r}}}{\partial \tilde{x}} + \breve{j}^{\mathrm{r}}$$
$$\bar{D}_{\mathrm{e}}^{\mathrm{left}}\frac{\partial \breve{c}_{\mathrm{e}}}{\partial \tilde{x}}\bigg|_{\mathrm{left}} = \bar{D}_{\mathrm{e}}^{\mathrm{right}}\frac{\partial \breve{c}_{\mathrm{e}}}{\partial \tilde{x}}\bigg|_{\mathrm{right}},$$

where "left" indicates a point and its corresponding cell region immediately to the left of a separator/electrode interface and "right" indicates a point and its cell region immediately to the right of the same interface. That is, at the negative-electrode/separator interface, left $= 1^{-}$ for the position and left $=$ n for the region; right $= 1^{+}$ for the position and right $=$ s for the region. Similarly, at the separator/positive-electrode interface, left $= 2^{-}$ for the position and

left = s for the region and right = 2^+ for the position and right = p for the region.

This set of definitions is perfectly correct, but we notice that the units of $\bar{n}_e^r$ are mol, and the parameter quantifies the total amount of lithium in the electrolyte in a certain cell region, scaled by the unitless constant $1 - t_+^0$. Ultimately, we will eliminate all units of mol from the model, retaining more common electrical units of amperes, volts, and ohms. As one step toward that goal, we define a new variable:[18]

$$\bar{q}_e^r = \frac{F}{3600}\bar{n}_e^r,$$

where $\bar{q}_e^r$ is now measured in ampere hours.[19] Then we can write

$$3600\bar{q}_e^r\frac{\partial \breve{c}_e^r}{\partial t} = F\frac{\partial}{\partial \tilde{x}}\bar{D}_e^r\frac{\partial \breve{c}_e^r}{\partial \tilde{x}} + F\breve{j}^r.$$

It appears that we now need also to find $\bar{q}_e^n$, $\bar{q}_e^s$, $\bar{q}_e^p$, $\bar{D}_e^n$, $\bar{D}_e^s$, and $\bar{D}_e^p$ in order to characterize a lithium-ion cell. However, note that there is a relationship between $\bar{D}_e^r$ and $\bar{\kappa}^r$ that we can exploit. Recall from Vol. I the definitions of effective conductivity and diffusivity in terms of the intrinsic conductivity and diffusivity:

$$\kappa_{eff}^n = \kappa(\varepsilon_e^n)^{brug}, \qquad D_{e,eff}^n = D_e(\varepsilon_e^n)^{brug},$$
$$\kappa_{eff}^s = \kappa(\varepsilon_e^s)^{brug}, \qquad D_{e,eff}^s = D_e(\varepsilon_e^s)^{brug},$$
$$\kappa_{eff}^p = \kappa(\varepsilon_e^p)^{brug}, \qquad D_{e,eff}^p = D_e(\varepsilon_e^p)^{brug},$$

where "brug" is the Bruggeman exponent. Therefore,[20]

$$F\frac{D_{e,eff}^n}{\kappa_{eff}^n} = F\frac{D_{e,eff}^s}{\kappa_{eff}^s} = F\frac{D_{e,eff}^p}{\kappa_{eff}^p} = F\frac{D_e}{\kappa}.$$

Similarly,[21]

$$F\frac{\bar{D}_e^n}{\bar{\kappa}^n} = F\frac{\bar{D}_e^s}{\bar{\kappa}^s} = F\frac{\bar{D}_e^p}{\bar{\kappa}^p} = \bar{\psi}T, \tag{1.25}$$

and if we have already identified the set of $\bar{\kappa}^r$, then we can compute the set of $\bar{D}_e^r$ by knowing only a single additional parameter, $\bar{\psi}$.

In summary, we rewrite the PDE, its boundary conditions, and initial condition as:

$$3600\bar{q}_e^r\frac{\partial \breve{c}_e^r}{\partial t} = \bar{\psi}T\frac{\partial}{\partial \tilde{x}}\bar{\kappa}^r\frac{\partial \breve{c}_e^r}{\partial \tilde{x}} + F\breve{j}^r$$
$$\bar{\kappa}^{left}\left.\frac{\partial \breve{c}_e^r}{\partial \tilde{x}}\right|_{left} = \bar{\kappa}^{right}\left.\frac{\partial \breve{c}_e^r}{\partial \tilde{x}}\right|_{right}$$
$$\breve{c}_e^r|_{left} = \breve{c}_e^r|_{right}$$
$$\breve{c}_{e,0}^r = 1.$$

Therefore, we now need also to find only $\bar{q}_e^n$, $\bar{q}_e^s$, $\bar{q}_e^p$, and $\bar{\psi}$.

[18] We admit that the constant of 3600 is cumbersome in the equations, but we believe that the final set of equations is less error-prone than if we had expressed $\bar{q}_e^r$ in coulombs.

[19] A physical interpretation of $\bar{q}_e^r$ is that it is the quantity of lithium in the electrolyte in region "r," divided by $(1 - t_+^0)$. We use the symbol "$\bar{q}_e$" to represent capacity or *quantity* of lithium in the electrolyte in ampere hours, much like we use Q to represent the capacity of the cell in ampere hours.

[20] In this analysis, we are assuming that κ_{eff}^r is uniform across each cell region. This is not true in general since κ_{eff}^r is in fact concentration-dependent and the concentration of lithium in the electrolyte varies across the cell. However, since we will enforce this assumption with the lab tests that we will develop to estimate model parameter values in Chap. 3 and we will employ the same assumption when creating reduced-order models in Chap. 4 (as we did in Vol. I), it causes no more harm to make the assumption at this point. To relax this assumption, one would need to replace $\bar{\psi}$ in the model with $\bar{D}_e^r$, as appropriate.

[21] In Chap. 3 we will use the Nernst–Einstein relationship to show that $\bar{D}_e^r/\bar{\kappa}^r$ is expected to be proportional to temperature T. Therefore, we factor out this temperature dependence here such that $\bar{\psi}$ is expected to be independent of temperature.

EQUATION V: The reaction-kinetics.

Finally, we consider the closure term of the model, expressed via Eqs. (1.19)–(1.21). We will not dwell on the details in this chapter since we will refine this model in Chap. 2 to add detail at the electrode/electrolyte boundary. For the time being, we insert the definitions we have created to this point:

$$\breve{j}^{\mathrm{r}} = \breve{j}_0^{\mathrm{r}} \left\{ \exp\left(\frac{(1-\alpha^{\mathrm{r}})F}{RT} \eta^{\mathrm{r}} \right) - \exp\left(\frac{-\alpha^{\mathrm{r}} F}{RT} \eta^{\mathrm{r}} \right) \right\}$$

$$\breve{j}_0^{\mathrm{r}} = \frac{k^{\mathrm{r}}_{\mathrm{norm},0}}{\bar{j}^{\mathrm{r}}} \left(\breve{c}_{\mathrm{e}}^{\mathrm{r}}\right)^{1-\alpha^{\mathrm{r}}} \left(1 - \frac{\breve{c}^{\mathrm{r}}_{\mathrm{s,e}}}{\bar{c}^{\mathrm{r}}_{\mathrm{s,max}}} \right)^{1-\alpha^{\mathrm{r}}} \left(\frac{\breve{c}^{\mathrm{r}}_{\mathrm{s,e}}}{\bar{c}^{\mathrm{r}}_{\mathrm{s,max}}} \right)^{\alpha^{\mathrm{r}}}$$

$$\eta^{\mathrm{r}} = \bar{\phi}^{\mathrm{r}}_{\mathrm{s}} \breve{\phi}^{\mathrm{r}}_{\mathrm{s}} - \bar{\phi}^{\mathrm{r}}_{\mathrm{e}} \breve{\phi}^{\mathrm{r}}_{\mathrm{e}} - U^{\mathrm{r}}_{\mathrm{ocp}}(\breve{c}^{\mathrm{r}}_{\mathrm{s,e}} / \bar{c}^{\mathrm{r}}_{\mathrm{s,max}}) - F\left[R^{\mathrm{r}}_{\mathrm{f}} \bar{j}^{\mathrm{r}}\right] j^{\mathrm{r}}.$$

We define $\bar{k}_0^{\mathrm{r}} = k^{\mathrm{r}}_{\mathrm{norm},0} / \bar{j}^{\mathrm{r}}$ and $\bar{R}^{\mathrm{r}}_{\mathrm{f}} = R^{\mathrm{r}}_{\mathrm{f}} \bar{j}^{\mathrm{r}}$. The additional parameter values we must then estimate are $\bar{k}_0^{\mathrm{n}}$, $\bar{k}_0^{\mathrm{p}}$, $\bar{R}^{\mathrm{n}}_{\mathrm{f}}$, $\bar{R}^{\mathrm{p}}_{\mathrm{f}}$, $\bar{\phi}^{\mathrm{n}}_{\mathrm{s}}$, α^{n}, and α^{p}.[22]

[22] Sometimes, we assume $\alpha^{\mathrm{r}} = 0.5$, which removes the requirement of finding α^{n} and α^{p}.

1.6 *Summary of reformulated model equations*

The process that we have followed has reduced the number of parameters that must be identified to characterize a physical lithium-ion cell from 36 down to 23 (21 if we assume $\alpha^{\mathrm{r}} = 0.5$). Thirteen "degrees of freedom" have been removed, making the parameter-estimation task mathematically possible in principle using only input/output current/voltage data. The lumped parameters of the reformulated model are summarized in Table 1.2 and in Sect. 1.A.4.

Table 1.2: Lumped parameters from the reformulated PDEs.

Negative electrode	Separator	Positive electrode
$\bar{\sigma}^{\mathrm{n}}$		$\bar{\sigma}^{\mathrm{p}}$
$\bar{\kappa}^{\mathrm{n}}$	$\bar{\kappa}^{\mathrm{s}}$	$\bar{\kappa}^{\mathrm{p}}$
$\bar{D}^{\mathrm{n}}_{\mathrm{s}}$		$\bar{D}^{\mathrm{p}}_{\mathrm{s}}$
$\bar{q}^{\mathrm{n}}_{\mathrm{e}}$	$\bar{q}^{\mathrm{s}}_{\mathrm{e}}$	$\bar{q}^{\mathrm{p}}_{\mathrm{e}}$
$\bar{k}^{\mathrm{n}}_0$		$\bar{k}^{\mathrm{p}}_0$
$\bar{R}^{\mathrm{n}}_{\mathrm{f}}$		$\bar{R}^{\mathrm{p}}_{\mathrm{f}}$
α^{n}		α^{p}
θ^{n}_0		θ^{p}_0
$\theta^{\mathrm{n}}_{100}$		$\theta^{\mathrm{p}}_{100}$
Q, $\bar{\kappa}_D$, and $\bar{\psi}$ span all regions		

Any similar formulation with the same number of parameters will also be minimal. Since some of the equations of the reformulated model are awkward, we slightly modify them to give a result that is easier to relate directly to the physical processes in the cell. The final notation we develop in this chapter is presented in Table 1.3 and is described below.

We consider first the equations that describe potential in the solid electrodes and the electrolyte. Analyzing the reformulated model shows that the constants $\bar{\phi}^{\mathrm{r}}_{\mathrm{s}}$ and $\bar{\phi}^{\mathrm{r}}_{\mathrm{e}}$ in all applicable cell regions must be estimated to solve for $\breve{\phi}^{\mathrm{r}}_{\mathrm{s}}$ and $\breve{\phi}^{\mathrm{r}}_{\mathrm{e}}$. Therefore, there is no benefit in converting the variables of the model from $\phi^{\mathrm{r}}_{\mathrm{s}}$ to $\breve{\phi}^{\mathrm{r}}_{\mathrm{s}}$ and from $\phi^{\mathrm{r}}_{\mathrm{e}}$ to $\breve{\phi}^{\mathrm{r}}_{\mathrm{e}}$. We choose to keep the original PDEs in terms of $\phi^{\mathrm{r}}_{\mathrm{s}}$ and $\phi^{\mathrm{r}}_{\mathrm{e}}$ but now written in terms of the new lumped-parameter values.

Considering the equations that describe lithium flux and concentrations in the solid electrodes and the electrolyte, we come to a different conclusion. After the reformulation, neither $\bar{c}^{\mathrm{r}}_{\mathrm{s}}$, $\bar{c}^{\mathrm{r}}_{\mathrm{e}}$, nor $\bar{j}^{\mathrm{r}}$ appear in the final PDEs, so we do not need to (nor can we) estimate these values from input/output data. So, for now, we will continue to write the corresponding PDEs as functions of $\breve{c}_{\mathrm{s}}$, $\breve{c}_{\mathrm{e}}$, and $\breve{j}$. However, we do note that the "breve" symbol in $\breve{j}$ becomes cumbersome,

Description	Governing equations	Boundary conditions	Initial conditions
Charge conservation in solid	$\bar{\sigma}^{\mathrm{r}} \frac{\partial^2 \phi_{\mathrm{s}}^{\mathrm{r}}}{\partial \tilde{x}^2} = i_{\mathrm{f}}^{\mathrm{r}}$	$\bar{\sigma}^{\mathrm{r}} \left.\frac{\partial}{\partial \tilde{x}} \phi_{\mathrm{s}}^{\mathrm{r}}\right\|_{\tilde{x}=0,3} = -i_{\mathrm{app}}$ $\bar{\sigma}^{\mathrm{r}} \left.\frac{\partial}{\partial \tilde{x}} \phi_{\mathrm{s}}^{\mathrm{r}}\right\|_{\tilde{x}=1,2} = 0$	$\phi_{\mathrm{s},0}^{\mathrm{p}} = U_{\mathrm{ocp}}^{\mathrm{p}}(\theta_{\mathrm{s},0}^{\mathrm{p}}) - U_{\mathrm{ocp}}^{\mathrm{n}}(\theta_{\mathrm{s},0}^{\mathrm{n}})$
Mass conservation in solid	$\frac{\partial \theta_{\mathrm{s}}^{\mathrm{r}}}{\partial t} = \frac{1}{\tilde{r}^2} \frac{\partial}{\partial \tilde{r}} (\bar{D}_{\mathrm{s}}^{\mathrm{r}} \tilde{r}^2 \frac{\partial \theta_{\mathrm{s}}^{\mathrm{r}}}{\partial \tilde{r}})$	$\bar{D}_{\mathrm{s}}^{\mathrm{r}} \left.\frac{\partial \theta_{\mathrm{s}}^{\mathrm{r}}}{\partial \tilde{r}}\right\|_{\tilde{r}=1} = -\frac{\left\|\theta_{100}^{\mathrm{r}} - \theta_0^{\mathrm{r}}\right\|}{10\,800 Q} i_{\mathrm{f}}^{\mathrm{r}}$ $\left.\frac{\partial \theta_{\mathrm{s}}^{\mathrm{r}}}{\partial \tilde{r}}\right\|_{\tilde{r}=0} = 0$	$\theta_{\mathrm{s},0}^{\mathrm{r}} = \theta_0^{\mathrm{r}} + z_0(\theta_{100}^{\mathrm{r}} - \theta_0^{\mathrm{r}})$
Charge conservation in electrolyte	$\frac{\partial}{\partial \tilde{x}} \left(\bar{\kappa}^{\mathrm{r}} \left(\frac{\partial}{\partial \tilde{x}} \phi_{\mathrm{e}}^{\mathrm{r}} + \bar{\kappa}_D T \frac{\partial \ln(\theta_{\mathrm{e}}^{\mathrm{r}})}{\partial \tilde{x}} \right) \right) + i_{\mathrm{f}}^{\mathrm{r}} = 0$	$\bar{\kappa}^{\mathrm{r}} \left(\frac{\partial}{\partial \tilde{x}} \phi_{\mathrm{e}}^{\mathrm{r}} + \bar{\kappa}_D T \frac{\partial \ln(\theta_{\mathrm{e}}^{\mathrm{r}})}{\partial \tilde{x}} \right) \Big\|_{\tilde{x}=1,2} = -i_{\mathrm{app}}$ $\bar{\kappa}^{\mathrm{r}} \left(\frac{\partial}{\partial \tilde{x}} \phi_{\mathrm{e}}^{\mathrm{r}} + \bar{\kappa}_D T \frac{\partial \ln(\theta_{\mathrm{e}}^{\mathrm{r}})}{\partial \tilde{x}} \right) \Big\|_{\tilde{x}=0,3} = 0$	$\phi_{\mathrm{e},0} = -U_{\mathrm{ocp}}(\theta_{\mathrm{s},0}^{\mathrm{n}})$
Mass conservation in electrolyte	$3600 \bar{q}_{\mathrm{e}}^{\mathrm{r}} \frac{\partial \theta_{\mathrm{e}}^{\mathrm{r}}}{\partial t} = \bar{\psi} T \frac{\partial}{\partial \tilde{x}} \bar{\kappa}^{\mathrm{r}} \frac{\partial}{\partial \tilde{x}} \theta_{\mathrm{e}}^{\mathrm{r}} + i_{\mathrm{f}}^{\mathrm{r}}$	$\bar{\kappa}^{\mathrm{n}} \left.\frac{\partial \theta_{\mathrm{e}}^{\mathrm{n}}}{\partial \tilde{x}}\right\|_{\tilde{x}=1^-} = \bar{\kappa}^{\mathrm{s}} \left.\frac{\partial \theta_{\mathrm{e}}^{s}}{\partial \tilde{x}}\right\|_{\tilde{x}=1^+}$ $\bar{\kappa}^{\mathrm{s}} \left.\frac{\partial \theta_{\mathrm{e}}^{\mathrm{s}}}{\partial \tilde{x}}\right\|_{\tilde{x}=2^-} = \bar{\kappa}^{\mathrm{p}} \left.\frac{\partial \theta_{\mathrm{e}}^{\mathrm{p}}}{\partial \tilde{x}}\right\|_{\tilde{x}=2^+}$ $\bar{\kappa}^{\mathrm{r}} \left.\frac{\partial \theta_{\mathrm{e}}^{\mathrm{r}}}{\partial \tilde{x}}\right\|_{\tilde{x}=0,3} = 0$	$\theta_{\mathrm{e},0} = 1$
Kinetics	$i_{\mathrm{f}}^{\mathrm{r}} = i_0^{\mathrm{r}} \left(\exp\left(\frac{(1-\alpha^{\mathrm{r}})F}{RT} \eta^{\mathrm{r}} \right) - \exp\left(\frac{-\alpha^{\mathrm{r}} F}{RT} \eta^{\mathrm{r}} \right) \right)$ $i_0^{\mathrm{r}} = \bar{k}_0^{\mathrm{r}} (\theta_{\mathrm{e}}^{\mathrm{r}})^{1-\alpha^{\mathrm{r}}} (1 - \theta_{\mathrm{s,e}}^{\mathrm{r}})^{1-\alpha^{\mathrm{r}}} (\theta_{\mathrm{s,e}}^{\mathrm{r}})^{\alpha^{\mathrm{r}}}$ $\eta^{\mathrm{r}} = \phi_{\mathrm{s}}^{\mathrm{r}} - \phi_{\mathrm{e}}^{\mathrm{r}} - U_{\mathrm{ocp}}^{\mathrm{r}}(\theta_{\mathrm{s,e}}^{\mathrm{r}}) - \bar{R}_{\mathrm{f}}^{\mathrm{r}} i_{\mathrm{f}}^{\mathrm{r}}$	$\tilde{x}=\{0,1,2,3\}$ at neg/current-collector, neg/sep, sep/pos, and pos/current-collector boundaries; $\tilde{r}=\{0,1\}$ at particle center and surface. Concentration ratios in solid and electrolyte are $\theta_{\mathrm{s}}=c_{\mathrm{s}}/c_{\mathrm{s,max}}$ and $\theta_{\mathrm{e}}=c_{\mathrm{e}}/c_{\mathrm{e},0}$; potentials in solid and electrolyte are ϕ_{s} and ϕ_{e}; flux is $i_{\mathrm{f}}=a_{\mathrm{s}} A L F j$. "Neg," "sep," and "pos" denoted by "n," "s," and "p"; "r"$\in$\{"n," "s," "p"\}.	

Table 1.3: Summary of the lumped-parameter version of the DFN model. *This is a preliminary result. We will refine this model and present an updated table in Chap. 2.* See Table 2.1.

so we rename $i_{\mathrm{f}} = F\check{j}$, recognizing that $\check{j}$ has units of $\mathrm{mol\,s^{-1}}$ and so the "faradaic current" i_{f} has units of amperes.[23] Recapping, the charge-conservation in the solid equation is presented in the first row of Table 1.3, where $\phi_{\mathrm{s}}^{\mathrm{r}}$ is measured in volts and $\bar{\sigma}^{\mathrm{r}}$ in siemens.

For the mass conservation in solid equation, $\bar{D}_{\mathrm{s}}^{\mathrm{r}}$ has units of $\mathrm{s^{-1}}$, which is manageable, but $\check{c}_{\mathrm{s}}^{\mathrm{r}}$ is in $\mathrm{mol\,s^{-1}}$, which is an awkward unit for concentration. We choose to rewrite its PDE in terms of the already-defined unitless $\theta_{\mathrm{s}}^{\mathrm{r}} = \check{c}_{\mathrm{s}}^{\mathrm{r}} / \check{c}_{\mathrm{s,max}}^{\mathrm{r}}$, which does not require finding any additional parameter values. For cleaner notation in the charge conservation in electrolyte relationship, we define a unitless ratio of concentrations, $\theta_{\mathrm{e}}^{\mathrm{r}} = \check{c}_{\mathrm{e}}^{\mathrm{r}}$. In these equations, $\phi_{\mathrm{e}}^{\mathrm{r}}$ is measured in volts, $\bar{\kappa}^{\mathrm{r}}$ in siemens, and t_+^0 is unitless. For the relationship describing mass conservation in the electrolyte, $\bar{q}_{\mathrm{e}}$ is in ampere hours and $\bar{\psi}$ is in volts per kelvin. For the kinetics equation, $\bar{k}_0^{\mathrm{r}}$ is in amperes, $\bar{R}_{\mathrm{f}}^{\mathrm{r}}$ is in ohms, and η^{r} is in volts. These modified equations are listed in the remaining four rows of the table.

Note that we will refine this model in Chap. 2. This table of equations is a preliminary result.

[23] Subscript "f" stands for "faradaic"; more on this in Chap. 2. Note that i_{f} is different from i_{app}, i_{s}, and i_{e}.

1.7 *Recovering original electrochemical variables*

The reformulated set of PDEs allows us to simulate $\phi_{\mathrm{s}}^{\mathrm{r}}$, $\phi_{\mathrm{e}}^{\mathrm{r}}$, $\theta_{\mathrm{s}}^{\mathrm{r}}$, $\theta_{\mathrm{e}}^{\mathrm{r}}$, and $i_{\mathrm{f}}^{\mathrm{r}}$, which is sufficient to be able to compute cell voltage.[24] However,

[24] This is why it is mathematically possible, in principle, to estimate the required parameter values from current/voltage input/output data.

what if we also desire the ability to simulate c_s^r, c_e^r, and j^r?

This will turn out not to be as necessary as it may seem. For example, cell absolute performance limits $0 \leq c_s^r \leq c_{s,max}^r$ automatically translate to $0 \leq \theta_s^r \leq 1$ without needing to simulate c_s^r directly or to estimate any new parameter values.

To recover all original parameter values and electrochemical variables from the modified set, we would need to be able to estimate ten additional coefficients: A, L^n, L^s, L^p, a_s^n, a_s^p, R_s^n, R_s^p, t_+^0, and $c_{e,0}$. It might seem that we should need to estimate thirteen values, since thirteen degrees of freedom have been removed from the model by the reduction process. However, two of those degrees of freedom were removed by noticing the relationship between $\bar{D}_e^r$ and $\bar{\kappa}^r$, which we summarized by replacing three $\bar{D}_e^r$ parameters with a single constant $\bar{\psi}$ in Eq. (1.25). The remaining degree of freedom was removed by noticing that operational capacity of both electrodes must be equal, which allowed us to replace two $\bar{c}_{s,max}^r$ parameters with a relationship involving the single constant Q in Eq. (1.24). Note that most of the ten remaining unknown values are physical dimensions and relatively easy to measure via cell teardown if needed. No fancy electrochemical techniques are required.

To recover all original electrochemical variables, if we are not concerned with recovering all original parameter values themselves, we would need to determine only eight additional values: $c_{s,max}^n$, $c_{s,max}^p$, $c_{e,0}$, a_s^n, a_s^p, L^n, L^p, and A.[25] Then we could compute:

$$c_s^r = c_{s,max}^r \theta_s^r$$
$$c_e^r = c_{e,0}^r \theta_e^r$$
$$j^r = \frac{i_f^r}{a_s^r A L^r F}.$$

[25] Note that we can combine the relationships from Sect. 1.5 to write:

$$c_{s,max}^r = \frac{10\,800 Q}{a_s^r A L^r R_s^r F |\theta_{100}^r - \theta_0^r|}.$$

Therefore, we can replace the requirement of finding $c_{s,max}^n$ and $c_{s,max}^p$ with the equivalent requirement of finding R_s^n and R_s^p, should those quantities prove to be simpler to measure in practice.

1.8 *Where to from here?*

We have now reformulated the DFN P2D physics-based PDE model of a lithium-ion cell to eliminate redundant parameters. The final form has a minimal number of unknown parameter values that must be determined to characterize a physical lithium-ion cell.

For BMS purposes, we need to convert this PDE model into a reduced-order state-space model. We will follow the same general procedure we introduced in Vol. I, but with some enhancements: First, we find transfer functions for each electrochemical variable. Next, we look at how to find parameter values for the model from laboratory tests. We then use a subspace realization algorithm to convert the transfer functions into reduced-order models. When we have done so, we will be able to simulate cells and packs given known pa-

rameter values. Then we have fully parameterized ROMs that can be used for BMS tasks such as SOC estimation, SOH estimation, power-limits estimation, and so forth.

We look at these topics in that order.

1.A Summary of variables

1.A.1 Notation conventions for variables and parameters

In this volume, we have attempted to name variables using a consistent format:

$$\mathrm{name}_{\mathrm{phase}}^{\mathrm{modifier,region}} \quad \text{or} \quad \mathrm{name}_{\mathrm{phase}}^{\mathrm{region}}.$$

- "name" is the variable identifier, such as ϕ for potential, θ for normalized concentration, and so forth.
- "modifier" is a temporary descriptive tag sometimes added during a derivation, but is not permanent (i.e., the modifier is eventually removed from the name).
- "region" is the cell domain to which this variable applies: either n, s, or p, for the negative electrode, separator, and positive electrode, respectively.
  - We sometimes leave the region blank; this usually means that an equation applies to multiple regions.
  - Sometimes the identifier "r" is given, showing more explicitly that the equation applies to multiple regions.
- "phase" is the material to which this variable applies, such as "s" for solid, "e" for electrolyte, "f" for film, and so forth.

We have also attempted to name constant parameters using a similar consistent format:

$$\overline{\mathrm{name}}_{\mathrm{phase}}^{\mathrm{modifier,region}} \quad \text{or} \quad \mathrm{name}_{\mathrm{phase}}^{\mathrm{modifier,region}}.$$

The presence of an overbar denotes a lumped parameter; the absence of an overbar denotes a standard parameter.

- "name" is the parameter identifier, such as κ for electrolyte conductivity.
- "region" and "phase" have the same interpretation as for variables.
- "modifier" is again a temporary descriptive tag sometimes added during a derivation, but is not permanent.